Characterisation of *Trichuris muris* secreted proteins and extracellular vesicles provides new insights into host-parasite communication

Ramon M. Eichenberger[a*], Md Hasanuzzaman Talukder[b*], Matthew A. Field[a], Phurpa Wangchuk[a], Paul Giacomin[a], Alex Loukas[a#], Javier Sotillo[a#]

[a]*Centre for Biodiscovery and Molecular Development of Therapeutics, Australian Institute of Tropical Health and Medicine, James Cook University, Cairns, QLD, Australia.*

[b]*Faculty of Veterinary Sciences, Bangladesh Agricultural University, Mymensingh-2202, Bangladesh*

[*] Both authors equally contributed to the manuscript

[#] Corresponding Authors:

Javier Sotillo. Centre for Biodiscovery and Molecular Development of Therapeutics, James Cook University, Cairns, 4878, Queensland, Australia. Email: javier.sotillo@jcu.edu.au

Prof. Alex Loukas. Centre for Biodiscovery and Molecular Development of Therapeutics, James Cook University, Cairns, 4878, Queensland, Australia. Email: alex.loukas@jcu.edu.au

Running title: Extracellular vesicles from *Trichuris muris*

Word count: 9,845

Abstract

Whipworms are parasitic nematodes that live in the gut of more than 500 million people worldwide. Due to the difficulty in obtaining parasite material, the mouse whipworm *Trichuris muris* has been extensively used as a model to study human whipworm infections. These nematodes secrete a multitude of compounds that interact with host tissues where they orchestrate a parasitic existence. Herein we provide the first comprehensive characterisation of the excretory/secretory products of *T. muris*. We identify 148 proteins secreted by *T. muris* and show for the first time that the mouse whipworm secretes exosome-like extracellular vesicles (EVs) that can interact with host cells. We use an Optiprep® gradient to purify the EVs, highlighting the suitability of this method for purifying EVs secreted by a parasitic nematode. We also characterise the proteomic and genomic content of the EVs, identifying >100 proteins, 56 miRNAs (22 novel) and 475 full-length mRNA transcripts mapping to *T. muris* gene models. Many of the miRNAs putatively mapped to mouse genes involved in regulation of inflammation, implying a role in parasite-driven immunomodulation. In addition, for the first time to our knowledge, we use colonic organoids to demonstrate the internalisation of parasite EVs by host cells. Understanding how parasites interact with their host is crucial to develop new control measures. This first characterisation of the proteins and EVs secreted by *T. muris* provides important information on whipworm-host communication and forms the basis for future studies.

Keywords: extracellular vesicles, exosomes, *Trichuris muris*, whipworm, miRNA, proteomics, organoids

1. Introduction

Infections with soil-transmitted helminths (STH) affect more than 1.5 billion people worldwide, causing great socio-economic impact as well as physical and intellectual retardation [1]. Among the STH, hookworms (*Necator americanus* and *Ancylostoma duodenale*), roundworms (*Ascaris lumbricoides*) and whipworms (*Trichuris trichiura*) are of particular importance due to their high prevalence and disease burden in impoverished countries [2]. For instance, *T. trichiura* alone infects around 500 million people worldwide, and contributes to 638,000 years of life lived with disability (YLDs) [2].

Infection with *Trichuris* spp. occurs after ingestion of infective eggs, which hatch in the caecum of the host. Larvae penetrate the mucosal tissue where they moult to become adult worms and reside for the rest of their lives. Due to the difficulty in obtaining parasite material to study whipworm infections, particularly adult worms, the rodent whipworm, *Trichuris muris*, has been extensively used as a tractable model of human trichuriasis [3, 4, 5]. In addition to parasitologists, immunologists have also benefited from the study of *T. muris* infections, and a significant amount of basic immunology research has been conducted using this model (reviewed by [6]). For instance, the role of IL-13 in resistance to nematode infections was elucidated using *T. muris* [7].

The recent publication of the genome and transcriptome of *T. muris* has provided meaningful insights into the immunobiology of whipworm infections [8]. This work provided new information on potential drug targets against trichuriasis and elucidated important traits that drive chronicity. Despite this progress, and the tractability of the *T. muris* model, very few proteomic studies have been conducted, and only a handful of reports have described proteins secreted by *Trichuris spp.* [9,

10, 11, 12, 13, 14]. Drake *et al*. characterised a pore-forming protein that *T. muris* [14] and *T. trichiura* [13] use to drill holes in the host cell membrane. Furthermore, it has been suggested that a thioredoxin-like protein secreted by the pig whipworm *Trichuris suis* plays a role in mucosal homeostasis [11].

The importance of excretory/secretory (ES) products in governing host-parasite interactions and ensuring parasite survival in inhospitable environments is indisputable. Traditionally, ES products were believed to contain only soluble proteins, lipids, carbohydrates and genomic content; however, the recent discovery of extracellular vesicles (EVs) secreted by helminths has revealed a new paradigm in the study of host-parasite relationships [15, 16, 17]. Helminth EVs have immunomodulatory effects and contribute to pathogenesis. For instance, EVs secreted by parasitic flatworms can promote tumorigenesis [18] and polarise host macrophages towards a M1 phenotype [19], while EVs from the gastrointestinal nematode *Heligmosomoides polygyrus* contain small RNAs that can modulate host innate immunity [20].

In the present study we aim to characterise the factors involved in *T. muris*-host relationships. We provide the first proteomic analysis of the soluble proteins present in the ES products and we describe the proteomic and nucleic acid content of EVs secreted by whipworms. This work provides important information on whipworm biology and contributes to the development of new strategies and targets to combat nematode infections in humans and animals.

2. Experimental procedures

2.1 Ethics statement

The study was approved by the James Cook University (JCU) Animal Ethics Committee (A2213). Mice were maintained at the JCU animal house (Cairns campus) under normal conditions of regulated temperature (22°C) and lighting (12 h light/dark cycle) with free access to pelleted food and water. The mice were kept in cages in compliance with the Australian Code of Practice for the Care and Use of Animals for Scientific Purposes.

2.2 Parasite material, isolation of ES products, and EV purification

Parasites were obtained from genetically susceptible B10.BR mice infected with 200 *T. muris* eggs. Adult worms were harvested from the caecum of infected mice 5 weeks after infection, washed in PBS containing 5× antibiotic/antimycotic (AA) and cultured for 5 days in RPMI containing 1× AA, at 37°C and 5% CO_2. The media obtained during the first 4 h after parasite culturing was discarded for further analysis. Dead worms were removed and ES products were collected daily, subjected to sequential differential centrifugation at 500 *g*, 2000 *g* and 4000 *g* for 30 min each to remove eggs and parasite debris. For the isolation of ES products, media was concentrated using a 10 kDa spin concentrator (Merck Millipore, USA) and stored at 1.0 mg/ml in PBS at -80°C until required.

For the isolation of EVs, the media obtained after differential centrifugation was processed as described previously [21]. Briefly, ES products were concentrated using a 10 kDa spin concentrator, followed by centrifugation for 45 min at 12,000 *g* to remove larger vesicles. A MLS-50 rotor (Beckman Coulter, USA) was used to ultracentrifuge the supernatant for 3 h at 120,000 *g* and the resultant pellet was resuspended in 70 µl of PBS and subjected to Optiprep® discontinous gradient (ODG) separation. One mL of 40%, 20%, 10% and 5% iodixanol solutions prepared

in 0.25 M sucrose, 10 mM Tris-HCl, pH 7.2, was layered in decreasing density in an ultracentrifuge tube, and the 70 µl containing the resuspended EVs was added to the top layer and ultracentrifuged at 120,000 *g* for 18 h at 4°C. Seventy (70) µl of PBS was added to the control tube prepared as described above. A total of 12 fractions were recovered from the ODG, and the excess Optiprep® solution was removed by buffer exchanging with 8 ml of PBS containing 1× EDTA-free protease inhibitor cocktail (Santa Cruz, USA) using a 10 kDa spin concentrator. The absorbance (340 nm) was measured in each of the fractions and density was calculated using a standard curve with known standards. The protein concentration of all fractions was measured using a Pierce BCA Protein Assay Kit (ThermoFischer, USA). All fractions were kept at -80°C until use.

2.3 Size and concentration analysis of EVs.

The size distribution and particle concentration of fractions recovered after ODG were measured using tunable resistive pulse sensing (TRPS) by qNano (Izon, USA) following the manufacturer's instructions. Voltage and pressure values were set to optimize the signal to ensure high sensitivity. A nanopore NP100 was used for all fractions analysed except for fraction 9, where a NP150 was used. Calibration was performed using CP100 carboxylated polystyrene calibration particles (Izon) at a 1:1000 dilution. Samples were diluted 1:5 and applied to the nanopore. The size and concentration of particles were determined using the software provided by Izon (version 3.2).

2.4 Exosome uptake in murine colonic organoids (mini-guts)

Murine colonic organoids were produced from intestinal crypts of a female C57 Bl6/J mouse according to previous reports [22] with some modifications. Briefly, murine colonic crypts were dissociated with Gentle Cell Dissociation reagent (Stemcell Technology Inc., Canada) and further incubated in trypsin (Gibco, ThermoFischer). Approximately 500 crypts were seeded in 50 µl of Matrigel (Corning, USA) in a 24-well plate and cultured in Intesticult Organoid Growth Medium (Stemcell Technology Inc.) supplemented with 100 ng/ml murine recombinant Wnt3a (Peprotech, USA). ROCK-inhibitor (10 µM Y-27632; Sigma-Aldrich, USA) was included in the culture medium for the first 2 days to avoid anoikis.

For imaging, organoids were seeded in 75 µl of Matrigel in 6-well plates and cultured for 7 days. To investigate internalization of EVs in the colonic epithelium layer, EVs were labelled with PKH26 (Sigma-Aldrich) according to the manufacturer's instructions. A total of 15-30 million stained particles (based on the TRPS results) in 3-5 µl were injected into the central lumen of individual organoids and cultured for 3 hours at 37°C and 4°C, respectively. Cell culture medium was removed, and wells were washed with PBS. Organoids were fixed by directly adding 4% paraformaldehyde to the 6-well plates and incubating for 30 min at room temperature (RT). Matrigel was then mechanically disrupted, and cells were transferred into BSA-coated tubes. Autofluorescence was quenched by incubating the organoids with 50 mM NH_4Cl in PBS (for 30 min at RT) and 100 mM glycine in PBS (for 5 min). Cell nuclei were stained with Hoechst dye (Invitrogen, US) and visualized using an AxioImager M1 ApoTome fluorescence microscope (Zeiss, Germany). Fluorescence intensity of PKH26-stained parasite EVs was quantified in ImageJ and expressed as percentage of corrected total fluorescence (% CTF) adjusted

by background fluorescence and the surveyed area in total epithelial cells (donut-shaped selection) or in the lumen incubated at different conditions in 10 different murine colonic organoids from 2 technical replicates (5 each).

2.5 Proteomic analyses

The protein content from the *T. muris* ES products and ODG fractions were analysed as follows.

2.5.1 Proteomic analysis of ES products

One hundred micrograms (100 µg) of *T. muris* ES proteins from two different batches of adult worms were precipitated at -20°C overnight in ice-cold methanol. Proteins were resuspended in 50 mM NH_4HCO_3, reduced in 20 mM dithiothreitol (DTT, Sigma-Aldrich) and finally alkylated in 55 mM iodoacetamide (IAM, Sigma-Aldrich). Proteins were finally digested with 2 µg of trypsin (Sigma-Aldrich) by incubating for 16 h at 37°C with gentle agitation. Reaction was stopped with 5% formic acid and the sample was desalted using ZipTip® (Merck Millipore). Both samples were kept at -80°C until use.

2.5.2 Proteomic analysis of the ODG fractions

For the proteomic analysis of ODG fractions, a total of 3 µg of protein from each ODG fraction was loaded on a 12% SDS-PAGE and electrophoresed at 100V for 1.5 h. The gel was stained using the Pierce Silver Staining Kit for Mass Spectrometry (ThermoFischer) as per manufacturer's instructions. Each lane was sliced into 4 pieces, which were subjected to trypsin digestion as described previously [23]. Briefly, each slice was washed for 5 min three times in 50% acetonitrile, 25 mM NH_4CO_3 and then dried under a vacuum centrifuge. Reduction was carried out in 20

mM DTT for 1 h at 65 °C, after which the supernatant was removed. Samples were then alkylated in 55 mM IAM at RT in darkness for 40 min. Gel slices were then washed 3× in 25 mM NH_4CO_3 before drying in a vacuum centrifuge followed by digestion with 500 ng of trypsin (Sigma-Aldrich) overnight at 37°C. The digest supernatant was removed from the gel slices, and residual peptides were removed from the gel slices by washing three times with 0.1% TFA for 45 min at 37°C. Samples were desalted and concentrated using Zip-Tip® and kept at -80°C until use.

2.5.2. Mass spectrometry and database searches

For all analyses, samples were reconstituted in 10 µl of 5% formic acid. Six microlitres of sample was injected onto a 50 mm 300 µm C18 trap column (Agilent Technologies, USA) and desalted for 5 min at 30 µL/min using 0.1% formic acid (aq). Peptides were then eluted onto an analytical nano HPLC column (150 mm x 75 µm 300SBC18, 3.5 µm, Agilent Technologies) at a flow rate of 300 nL/min and separated using a 35 min gradient of 1-40% buffer B (90/10 acetonitrile/ 0.1% formic acid) followed by a steeper gradient from 40-80% buffer B in 5 min. The mass spectrometer operated in information-dependent acquisition mode (IDA), in which a 1-s TOF MS scan from 350-1400 m/z was performed, and for product ion ms/ms 80-1400 m/z ions observed in the TOF-MS scan exceeding a threshold of 100 counts and a charge state of +2 to +5 were set to trigger the acquisition of product ion. Analyst 1.6.1 (ABSCIEX) software was used for data acquisition and analysis.

A database was built using the *T. muris* genome [8] with the common repository of adventitious proteins (cRAP, http://www.thegpm.org/crap/) appended to it. Database search was performed using X!Tandem, MS-GF+, OMSSA and Tide search engines using SearchGUI [24]. Parameters were set as follows: tryptic

specificity allowing two missed cleavages, MS tolerance of 50 ppm and 0.2 Da tolerance for MS/MS ions. Carbamidomethylation of Cys was used as fixed modification and oxidation of Met and deamidation of Asn and Gln as variable modifications. PeptideShaker v.1.14.1 was used to import the results for peptide and protein inference [25]. Only proteins with a false discovery rate <1% having at least two unique peptides (containing at least seven amino acid residues) were considered as positively identified.

2.6. RNA analyses

2.6.1. mRNA and miRNA isolation

Two different biological replicates of EVs obtained from two different batches of worms were used. ODG fractions with a density between 1.06 and 1.08 (fractions containing pure EV samples after TRPS analysis) were pooled and excess Optiprep® solution was removed by buffer exchanging. Total RNA and miRNA were extracted using the mirVana™ miRNA Isolation Kit (ThermoFischer) according to the manufacturer's instructions. RNA was eluted over two fractions of 50 µl each and stored at -80°C until analysed.

2.6.2. RNA sequencing and transcript annotation

The RNA quality, yield, and size of total and small RNAs were analyzed using capillary electrophoresis (Agilent 2100 Bioanalyzer, Agilent Technologies, USA). Ribosomal RNA was removed from samples, which were pooled for sufficient input material for further sequencing, resulting in one sample for mRNA and two samples for miRNA analyses, respectively. mRNA and miRNA were prepared for sequencing using Illumina TruSeq stranded mRNA-seq and Illumina TruSeq Small RNA-seq

library preparation kit according to the manufacturer's instructions, respectively. RNAseq was performed on a HiSeq 500 (Illumina, single-end 75-bp PE mid output run, approx. 30M reads per sample). Quality control, library preparation and sequencing were performed at the Ramaciotti Centre for Genomics at the University of New South Wales.

2.7 Bioinformatic analyses

2.7.1 Proteomics

Proteins were classified according to Gene Ontology (GO) categories using the software Blast2GO basic version 4.0.7. [26] and Pfam using HMMER v3.1b1 [27]. Putative signal peptides and transmembrane domain(s) were predicted using the programs CD-Search tool [28] and SignalP [29].

2.7.2. mRNA analysis

High-throughput RNA-seq data was aligned to the *T. muris* reference genome models (WormBase WS255; http://parasite.wormbase.org; [30]) using the STAR transcriptome aligner [31]. Prior to downstream analysis, rRNA-like sequences were removed from the metatranscriptomic dataset using riboPicker-0.4.3 (http://ribopicker.sourceforge.net; [32]). BLASTn algorithm [33] was used to compare the non-redundant mRNA dataset for *T. muris* EVs to the nucleotide sequence collection (nt) from NCBI (www.ncbi.nlm.nih.gov) to identify putative homologues in a range of other organisms (cut-off: <1E-03). Corresponding hits homologous to the murine host, with a transcriptional alignment coverage <95% (based on the effective transcript length divided by length of the gene), and with an expression level <10 fragments per kilobase of exon model per million mapped reads

(FPKM) normalized by the length of the gene, were removed from the list. The final list of mRNA transcripts from *T. muris* exosomes was assigned to protein families (Pfam) and GO categories (Blast2GO).

2.7.3. miRNA analysis and target prediction

The miRDeep2 package [34] was used to identify known and putative novel miRNAs present in both miRNA samples. As there are no *T. muris* miRNAs available in miRBase release 21 [35], the miRNAs from the nematodes *Ascaris suum*, *Brugia malayi*, *Caenorhabditis elegans*, *Caenorhabditis brenneri*, *Caenorhabditis briggsae*, *Caenorhabditis remanei*, *Haemonchus contortus*, *Pristionchus pacificus*, *Panagrellus redivivus*, and *Strongyloides ratti* were utilised as a training set for the algorithm. Only miRNA sequences commonly identified in both replicates were included for further analyses. The interaction between miRNA and murine host genes was predicted using the miRanda algorithm 3.3a [36]. Input 3'UTR from the *Mus musculus* GRCm38.p4 assembly was retrieved from the Ensembl database release 86 [37]. The software was run with strict 5' seed pairing, energy threshold of -20 kcal/mol and default settings for gap open and gap extend penalties. Interacting hits were filtered by conservative cut-off values for pairing score (>155) and matches (>80%). The resulting gene list was classified by the Panther classification system (http://pantherdb.org/) using pathway classification [38] and curated by the reactome pathway database (www.reactome.org) [39].

3. Results

3.1 Proteomics analysis of the ES products of T. muris

The ES products secreted by two different batches of *T. muris* adult worms were analysed using LC-MS/MS. A total of 1,777 and 2,056 peptide-spectrum matches (PSMs) were confidently identified in the first and second biological replicates analysed respectively. Similarly, a total of 591 and 704, corresponding to 197 and 233 proteins were identified with 100% confidence. After removing the proteins identified from only one peptide and the sequences belonging to the contaminants, 100 and 116 *T. muris* proteins were identified in both replicates. A total of 68 proteins were found in both replicates, whereas 32 and 48 proteins were uniquely found in replicate 1 and 2 respectively, resulting in 148 proteins in total (Supplementary Table 1).

The identified proteins were subjected to a Pfam and GO analysis. The most represented domains were “trypsin-like peptidase”, “thioredoxin-like” and “tetratricopeptide repeat domains”, with 21, 19 and 13 proteins containing these domains respectively (Figure 1A). The most abundant GO terms within the “molecular function” ontology were “protein binding”, “metal ion binding” and “nucleic acid” as well as “isomerase activity”, “oxidoreductase activity” and “serine-type peptidase activity” (Figure 1B). The GO terms within “biological process” and “cell component” (as well as the above mentioned “molecular function”) are detailed in Supplementary Table 1.

From the total of 148 proteins found in both replicates, only 62 had a signal peptide (Supplementary Table 2), which opened the possibility of other non-classical mechanisms of secretion of these proteins described in other helminths, such as EVs.

3.2 T. muris adult worms secrete exosome-like EVs that can be internalised by host cells

The ES products secreted by *T. muris* adult worms were concentrated and EVs purified using Optiprep® gradient. The density of the 12 fractions recovered after Optiprep® separation was measured, ranging from 1.04-1.27 g/ml (Table 1). All fractions were subjected to TRPS analysis using a qNano system, but only fractions 4-10 contained enough vesicles for the analysis (Figure 2). Fraction 6 (corresponding to a density of 1.07 g/ml) contained the highest number of EVs (1.34×10^{-12} particles/ml), followed by fractions 7 (density = 10.08 g/ml; concentration = 8.21×10^{-10} particles/ml) and fraction 5 (density = 1.07 g/ml; concentration = 7.47×10^{-10}) (Table 1). Protein concentration was measured in all fractions, and EV purity determined as described previously [40] (Table 1). Fraction 6 had the purest EV preparation (4.31×10^{-9} particles/µg), followed by Fractions 7 and 5 (4.04×10^{-08} and 1.58×10^{-08} particles/µg respectively) (Table 1). Furthermore, the vesicle size was determined using the qNano system, and the results are summarised in Table 1.

Cellular uptake of membrane-stained *T. muris* EVs was demonstrated in murine colonic organoids (Figure 3). Fluorescence micrographs after 3 hours of culture present a cytoplasmic location of the stained EVs in some cells within the donut-shaped epithelial layer, representing EV uptake at 37°C. The EVs appear to cluster at the mucosal cell surface at 4°C, suggestive of a specific cell interaction (Figure 3A, B). Three hours after EV injection into the central lumen, at 37°C, stained vesicles could be traced within a small subset of epithelial organoid cells (mean corrected total fluorescence intensity (CTF) +/-SD: 4.04 +/- 1.11), and CTF values were significantly reduced ($p<0.001$) in the central lumen (0.59 +/- 0.41), whereas at 4°C, CTF values were 0.21 +/- 0.29 and 3.79 +/-2.29 for the total epithelial organoid cells and the central lumen, respectively (Figure 3C).

3.3 T. muris secreted EVs contain specific proteins

All 12 fractions after ODG were subjected to SDS-PAGE separation, each lane cut into 4 slices and subjected to trypsin digestion followed by LC-MS/MS analysis. The results obtained from fractions 5-7 (fractions containing the purest EV samples) were combined and subjected to protein identification analysis. Although fractions 4 and 8 contained a significant amount of EVs, they were not included in the analysis to avoid potential contamination with soluble proteins. A total of 11,201 spectra corresponding to 1,100 peptides were identified. A total of 225 proteins matching *T. muris*, *M. musculus* and common contaminants for the cRAP database were identified (Supplementary Table 3), and, a final list of 103 and 15 proteins corresponding to *T. muris* and *M. musculus* respectively was defined with proteins identified with ≥2 unique peptides (Supplementary Table 4).

Among the identified proteins from *T. muris*, the most abundant proteins based on the spectrum count were a poly-cysteine and histidine-tailed protein, several sperm-coating protein (SCP)-like extracellular proteins, also called SCP/Tpx-1/Ag5/PR-1/Sc7 domain containing proteins (SCP/TAPS), a glyceraldehyde-3-phospahte dehydrogenase and a fructose-bisphosphate aldolase. Strikingly, tetraspanins which are abundant markers of exosomes, were absent from our dataset, but other proteins typically found in EVs from helminths like enolase, 14-3-3, heat shock protein (HSP) and glutathione-s-transferase were also identified in this study. Furthermore, from the 103 identified proteins from *T. muris*, only 13 (12.6%) contained a transmembrane domain, and 37 (35.9%) had a signal peptide. Despite washing the worms extensively before culturing, discarding the first 4 hours of the ES for EV isolation (which typically contains a significant amount of host proteins) and analysing only fractions containing highly pure EV samples, we found some host

373 proteins in our analysis. Among these proteins we found histones, keratins, albumin,
374 antibodies and mucin-2 (Supplementary Table 4).

375 Following a GO analysis, the most represented GO terms within biological
376 process in the *T. muris* EV proteins were assigned as “proteolysis”, “cellular protein
377 metabolic process” and “oxidation-reduction process” (Figure 4A). Similarly, the
378 most represented GO terms within molecular function were “protein binding”, “kinase
379 activity” and serine-type endopeptidase activity” (Figure 4B).

380

381 *3.4 T. muris secreted EVs contain specific mRNAs and miRNAs*

382 RNA content of EVs was characterized using the Illumina HiSeq platform. For
383 an initial description of parasite-specific mRNAs in EVs, total RNA from a highly
384 pure EV sample was sequenced and results were curated based on stringent
385 thresholds. This resulted in 475 full-length mRNA transcripts mapping to *T. muris*
386 gene models. The identified hits were subjected to a Pfam and GO analysis.
387 Interestingly, the most represented domains were of “unknown function”, “reverse
388 transcriptase”, and “helicase”, whereas other gene models with DNA-binding and
389 processing domains were also highly abundant (e.g. genes with “retrotransposon
390 peptidase” domain) (Figure 5A). Mapping to molecular functions identified “protein
391 binding” as the most abundant term, with 31.9% of all sequences involved in this
392 function (Figure 5B). The underlying proteins from the parasite-specific mRNAs had
393 functions in signalling and signal transduction, transport, protein modification and
394 biosynthetic processes, as well as in RNA processing and DNA integration (Figure
395 5C). Data is provided in Supplementary Table 5.

396 By sequencing and screening biological duplicates for miRNAs, we identified
397 56 miRNAs commonly present in both datasets, with 34 having close homologs in

other nematodes. The remaining 22 miRNAs were novel and were named serially according to their mean abundances (tmu.miR.ev1 to tmu.miR.ev22). Potential interactions of *T. muris* miRNAs to murine host genes were explored by computational target prediction. The 56 nematode EV-miRNAs were predicted to interact with 2,043 3'UTR binding sites of the mouse genome assembly (Supplementary Table 6). Associated annotated coding genes were grouped according to signalling, metabolic, and disease pathways (Supplementary Figure 1). Indeed, a number of the nematode miRNA-mouse gene interactions are involved in host immune system, receptor, and transcriptional regulation (Figure 6). Within the 56 identified EV miRNAs, 3 (5.4%) could not be assigned for interaction with a specific pathway in the murine host, including the second most abundant asu-miR-5360-5p.

4. Discussion

Trichuriasis is a soil transmitted helminth infection that affects almost 500 million people worldwide [1, 41, 42]. In addition to the pathogenicity associated with the disease, the infection can also cause physical and intellectual retardation [1, 43]. There is, therefore, an urgent need to understand the mechanisms by which the parasite interacts with its host such that novel approaches to combat this neglected tropical disease can be developed [44]. *T. trichiura* is the main species that affects humans, but the difficulty in obtaining worms and working with the adult stage have prompted parasitologists and immunologists to use the *T. muris* rodent model.

We provide herein the first high throughput study of the secretome of *T. muris*. The analysis of the genome from *T. muris* predicted 434 proteins containing signal peptides [8]. We have confidently identified (with 2 or more peptides) 148 proteins secreted by adult *T. muris*, corresponding to 34.1% of the total predicted

423 secreted proteins [8]). From the total proteins identified, 68 were commonly found in
424 both replicates, highlighting the importance of analysing multiple batches of samples
425 when conducting proteomics analyses of parasitic ES products. Among the identified
426 proteins we found several peptidases and proteases (such as serine proteases, pepsin
427 and trypsin domain-containing proteins) and also protease inhibitors including WAP
428 domain-containing proteins. These findings are in agreement with the functional
429 annotation of the *T. muris* proteins predicted from the genome [8]. Protease inhibitors
430 (particularly serine protease inhibitors and secretory leukocyte proteinase inhibitor
431 (SLPI)-like proteins - proteins containing mostly WAP domains) are abundantly
432 represented in the *T. muris genome* [8]. SLPI-like proteins have been suggested to
433 have immunomodulatory properties as well as a role in wound healing [8, 45, 46, 47],
434 so they could be secreted in an attempt to modulate the host's immune response and
435 repair damage caused by both feeding/migrating worms and immunopathogenesis. In
436 addition, we found five SCP/TAPS (also known as CAP-domain) proteins.
437 SCP/TAPS proteins are abundantly represented in soil-transmitted helminths,
438 although they have not been well characterised in the clade I nematodes [48].

439 Only recently, different authors have shown the importance of helminth-
440 secreted EVs in host-parasite interactions. The secretion of small EVs was
441 demonstrated in various intracellular and extracellular parasites, interacting with their
442 hosts in a specific manner (reviewed in [17]). In addition, the secretion of EVs has
443 been demonstrated thus far only in a small number of nematodes, including the free-
444 living *C. elegans*, the filarial nematodes *Brugia malayi* and *Dirofilaria immitis*, the
445 rodent nematode *Heligmosomoides polygyrus* and the ovine and porcine intestinal
446 nematodes *Teladorsagia circumcincta* and *Trichuris suis*, respectively [20, 49, 50, 51,
447 52].

448 Our results show that *T. muris* secretes EVs with a wide variety of sizes (40-
449 550 nm). In order to study the exosome-like vesicles (vesicles with a size between 50-
450 150 nm) and eliminate contamination with soluble proteins that could be co-
451 precipitated in the ultracentrifugation step, we further purified the EVs using Optiprep
452 and analysed only fractions 5-7 (fractions containing EVs with sizes between
453 72±23.8nm to 90±25.5nm). For a totally novel approach in EV research, we
454 introduced and established a long-term primary *in vitro* culture to generate 3D
455 intestinal organoids, recapitulating the *in vivo* epithelial tissue organisation and
456 representing the complete census of progenitors (stem cells) and differentiated cells
457 [22, 53]. Although there are colonic cancer cell lines available, such as the intestinal
458 epithelial cell line Caco2, cell lines cannot recapitulate the complex spatial
459 organisation of the intestinal epithelium, they have undergone significant molecular
460 changes to become immortal, and do not represent all intestinal subsets [54]. Hence,
461 we used colonic organoids corresponding to the epithelial barrier, which is the first
462 line of defence against intestinal pathogens. We observed EV uptake only in a subset
463 of the cells, which we have yet to characterise. Interestingly at 4°C (metabolically
464 inactive state of the cells), the EVs seem to assemble and adhere to the luminal
465 surface of the organoids, suggesting a specific cell interaction. A disadvantage of the
466 intestinal organoid culture is the lack of any immune cells. Co-culture experiments
467 with intestinal organoids and intraepithelial lymphocytes as described by Nozaki and
468 colleagues [55] could be a powerful tool to study interactions of EVs with immune
469 cells at their primary interface.

470 The proteomic analysis of the exosome-like EVs showed a total of 118
471 proteins (103 from *T. muris* and 15 from the host), 67 of which have been also found
472 in the crude ES prep. From the common proteins, only 27 (40%) were predicted to

have a signal peptide, thus, EVs could be a potential mechanism by which these proteins are secreted by helminths into the extracellular milieu, addressing an issue that has been frequently debated in the literature [8]. It is interesting to note that no tetraspanins were detected in the *T. muris* EVs. Tetraspanins are considered a molecular marker of exosomes since they are present on the surface membrane of EVs from many different organisms including mammalian cells and bacteria [56]. EVs secreted by, or shed from the surface of parasitic trematodes are enriched in tetraspanins [18, 21, 57], but in the case of nematodes, only *H. polygyrus* has been shown to secrete EVs containing tetraspanins, although only one member was found [20]. However, the EVs from *H. polygyrus* were not purified after ultracentrifugation, which makes it difficult to compare this protein dataset with our own from *T. muris*. The *T. muris* genome contains 23 genes encoding for proteins with a tetraspanin domain (domain E-value <0.05), which indicates that this family of proteins is present in the parasite, although might not be important for exosome biogenesis in this group of parasites. Since tetraspanins are also involved in the formation of the membrane of EVs [56], it is unclear why EVs secreted by nematode parasites are not replete in tetraspanins. Tetraspanins were also absent in the exosomes secreted by other nematodes such as *B. malayi* and *T. circumcincta* [52, 58], which leads us to hypothesize that in helminths, the presence of tetraspanins in exosome-like vesicles is a hallmark of trematode flatworms but not of nematode roundworms. In trematodes, exosomes derive from the tegumental syncytium of the worm [59], whereas in nematodes they seem to have an intestinal origin [20]. This different origin could be the reason why tetraspanins are not enriched in nematode EVs. Despite the absence of tetraspanins, our dataset presents other proteins usually found in parasitic exosomes, such as 14-3-3, enolase and myoglobin.

Proteins involved in proteolysis were abundantly represented (16.5% of sequences) in the *T. muris* EVs (e.g. trypsin like and pepsin proteins). *Trichuris* lacks the muscular pharynx that many other nematodes use to ingest their food, a challenging process given the hydrostatic pressure of the pseudocoelom that characterizes the phylum. Instead, it has been suggested that the parasite secretes copious quantities of digestive enzymes for this purpose [8]. We have shown that proteases are heavily represented in the ES products, and proteolysis is also the main GO term found when we analysed the proteins present in the EVs. Indeed, 10 of the 103 proteins from *T. muris* found in the EVs contain a trypsin domain. These proteins could be involved in extracellular digestion, and, since feeding is a key process in parasite biology, they might also be potential targets for vaccines and drugs against the parasite. Helminth proteases have also been hypothesized to be involved in immunomodulatory processes, where they degrade important immune cell surface receptors [60] and host intestinal mucins [9, 61]. If this is the case, *Trichuris* could be secreting EVs containing peptidases to promote an optimal environment for attaching to the mucosa and feeding purposes.

Proteins containing an SCP/TAPS domain were identified in the EVs secreted by *T. muris*. This family of proteins is abundantly expressed by parasitic nematodes and trematodes. For instance, they represent at least 28% of the ES products of the hookworm *Ancylostoma caninum*, and have been found in free-living and plant nematodes (reviewed by [62]). Their role is still unknown, although they have been suggested to play roles in fundamental biological processes such as larval penetration [63], modulation of the immune response [64, 65], in the transition from the free-living to the parasitic stage [66] and have even been explored as vaccine candidates against hookworm infections [67]. It is interesting to note that EVs from other

helminths are enriched for many known vaccine candidate antigens [21]. Since SCP/TAPS proteins are abundant in the EVs secreted by *T. muris*, their potential use as vaccines should be further explored.

The presence of contaminating host proteins in parasite EV preps is an unavoidable concern when the parasite developmental stage of interest can only be acquired from the host. We found 15 host (mouse) proteins in the *T. muris* EV preps. When we analysed the different fractions after Optiprep gradient using a proteomics approach, we found several differences depending on the proteins. For instance, albumin is present in fractions 1-8 except in fraction 6 (which is, interestingly, the fraction with the highest purity of EVs), which suggests that its presence could be due to a contamination after ultracentrifugation, a phenomenon initially identified from the mammalian exosome literature [68]. Similarly, mouse galectin-3 is present throughout the fractions except in fractions 4, 11 and 12, suggesting, again, that its presence could be due to co-precipitation (eg. binding to exosome surface glycans) during the ultracentrifugation step. Mucin-2 was only present in fractions 4-9, which are the fractions containing EVs (fractions 5-7 had the highest purity, but 4, 8 and 9 were also found to contain EVs). Mucins have been shown to be key in maintaining the structure of EVs secreted by human tracheobronchial epithelial cells [69]. We therefore hypothesize that mouse mucin-2 binds to *T. muris* EV proteins such as galactoside-binding protein where it might facilitate initial binding of *T. muris* EVs to colonic epithelial cells, although further work is needed to confirm this theory.

We analysed the mRNA and miRNA content of the exosome-like EVs secreted by *T. muris* since it has been well documented that the nucleic acid content of eukaryotic EVs can be delivered between species to other cells, and can be functional in the new location [70]. Functional categorization of the 475 mRNAs from *T. muris*

548 EVs revealed a high proportion of protein-binding proteins. Interestingly, mRNAs for
549 common EV proteins were present, including inter alia mRNAs for tetraspanins,
550 HSPs, histones, ubiquitin-related proteins, and signalling- and vesicle trafficking
551 molecules (rab, rho and ras). A significant number of domains found in the proteins
552 predicted from mRNA sequences were involved in reverse transcription and
553 retrotransposon activity, suggesting a strong involvement of these mRNAs in direct
554 interactions with the host target cell genome. This is supported by the hypothesis of
555 shared pathways between EV biogenesis and retrovirus budding, including the
556 molecular composition of the released particles, sites of budding in different cell
557 types, and the targeting signals that deliver proteins [71, 72, 73, 74].

558 To gain a more comprehensive picture of the RNA composition of the *T.*
559 *muris* EVs, we sequenced the miRNAs present in *T. muris* EVs and identified 56
560 miRNAs, including 22 novel miRNAs without described homology to other
561 nematodes. We also identified miRNAs that shared homology with those from other
562 parasitic nematodes, such as let-7, miR-2, miR-9, miR-34, miR-36 (a and c), miR-44,
563 miR-60, miR-72, miR-81, miR-86, miR-87, miR-92, miR-228, miR-236 and miR-252
564 (reviewed in [75]). This suggests that secretion of miRNAs by parasitic nematodes is
565 most probably conserved and that EVs could be playing an important role in this
566 secretory pathway. *T. muris* miRNAs that regulate expression of genes involved in
567 specific conditions and cellular pathways were identified. In humans, more than 60%
568 of all protein-coding genes are thought to be controlled by miRNAs (reviewed in
569 [76]). Our *in silico* prediction analysis of murine host gene interactions of *T. muris*
570 EV miRNAs points towards a strong involvement of parasite miRNAs in
571 regulation/modulation of the host immune system [77]. In this sense, it has been
572 previously demonstrated that small EVs secreted by *H. polygyrus* interact with

intestinal epithelial cells of its murine host and suppress type 2 innate immune responses, promoting parasite survival [20]. Similarly, other studies demonstrated the secretion of EVs containing miRNAs by larvae of the porcine whipworm *T. suis*, and although the miRNAs were not sequenced, the authors suggested a possible role in immune evasion [49].

The mechanisms by which parasitic helminths pack their nucleic acid cargo into EVs is still unknown, and, while we hypothesize that an active mechanism might regulate this process, we cannot discard the possibility that mRNAs and miRNAs could be internalised at random. Understanding this mechanism will be of importance in understanding the intimately interactive nature of host-parasite biology. For example, are mRNAs in parasite EVs translated into protein by target host cells, akin to viral hijacking of host cell protein manufacturing machinery? Or, are EV mRNAs unimportant, and manipulation of host cell gene expression is mostly due to miRNAs?

In the present study we have provided important information regarding the molecules secreted by the murine whipworm *T. muris*. The identification of the secreted proteins and EVs (including their proteomic and RNA content) will prove useful not only for the design of novel approaches aimed at controlling whipworm infections, but also to understand the way the parasite promotes an optimal environment for its survival.

Funding

This work was supported by a program grant from the National Health and Medical Research Council (NHMRC) [program grant number 1037304] and a Principal Research fellowship from NHMRC to AL. RME was supported by an Early Postdoc Mobility Fellowship (P2ZHP3_161693) from the Swiss National Science

598 Foundation. MHT was supported by an Endeavour Research Fellowship. The funders
599 had no role in study design, data collection and analysis, decision to publish, or
600 preparation of the manuscript. The authors declare no competing financial interests.

601

602 **References**
603

604 1. Bethony J, Brooker S, Albonico M, Geiger SM, Loukas A, Diemert D, Hotez
605 PJ. Soil-transmitted helminth infections: ascariasis, trichuriasis, and hookworm.
606 Lancet. 2006;367:1521-32.
607 2. Pullan RL, Smith JL, Jasrasaria R, Brooker SJ. Global numbers of infection
608 and disease burden of soil transmitted helminth infections in 2010. Parasit Vectors.
609 2014;7:37.
610 3. Klementowicz JE, Travis MA, Grencis RK. *Trichuris muris*: a model of
611 gastrointestinal parasite infection. Semin Immunopathol. 2012;34:815-28.
612 4. Cliffe LJ, Grencis RK. The *Trichuris muris* system: a paradigm of resistance
613 and susceptibility to intestinal nematode infection. Adv Parasitol. 2004;57:255-307.
614 5. Bancroft AJ, Hayes KS, Grencis RK. Life on the edge: the balance between
615 macrofauna, microflora and host immunity. Trends Parasitol. 2012;28:93-8.
616 6. Hurst RJ, Else KJ. *Trichuris muris* research revisited: a journey through time.
617 Parasitology. 2013;140:1325-39.
618 7. Grencis RK, Bancroft AJ. Interleukin-13: a key mediator in resistance to
619 gastrointestinal-dwelling nematode parasites. Clin Rev Allergy Immunol. 2004;26:51-
620 60.
621 8. Foth BJ, Tsai IJ, Reid AJ, Bancroft AJ, Nichol S, Tracey A, Holroyd N,
622 Cotton JA, Stanley EJ, Zarowiecki M, Liu JZ, Huckvale T, Cooper PJ, Grencis RK,
623 Berriman M. Whipworm genome and dual-species transcriptome analyses provide

molecular insights into an intimate host-parasite interaction. Nat Genet. 2014;46:693-700.

9. Hasnain SZ, McGuckin MA, Grencis RK, Thornton DJ. Serine protease(s) secreted by the nematode *Trichuris muris* degrade the mucus barrier. PLoS Negl Trop Dis. 2012;6:e1856.

10. Laan LC, Williams AR, Stavenhagen K, Giera M, Kooij G, Vlasakov I, Kalay H, Kringel H, Nejsum P, Thamsborg SM, Wuhrer M, Dijkstra CD, Cummings RD, van Die I. The whipworm (*Trichuris suis*) secretes prostaglandin E2 to suppress proinflammatory properties in human dendritic cells. FASEB J. 2016.

11. Ditgen D, Anandarajah EM, Hansmann J, Winter D, Schramm G, Erttmann KD, Liebau E, Brattig NW. Multifunctional thioredoxin-like protein from the gastrointestinal parasitic nematodes *Strongyloides ratti* and *Trichuris suis* affects mucosal homeostasis. J Parasitol Res. 2016;2016:8421597.

12. Santos LN, Gallo MB, Silva ES, Figueiredo CA, Cooper PJ, Barreto ML, Loureiro S, Pontes-de-Carvalho LC, Alcantara-Neves NM. A proteomic approach to identify proteins from *Trichuris trichiura* extract with immunomodulatory effects. Parasite Immunol. 2013;35:188-93.

13. Drake LJ, Barker GC, Korchev Y, Lab M, Brooks H, Bundy DA. Molecular and functional characterization of a recombinant protein of *Trichuris trichiura*. Proc Biol Sci. 1998;265:1559-65.

14. Drake L, Korchev Y, Bashford L, Djamgoz M, Wakelin D, Ashall F, Bundy D. The major secreted product of the whipworm, Trichuris, is a pore-forming protein. Proc Biol Sci. 1994;257:255-61.

15. Marcilla A, Trelis M, Cortes A, Sotillo J, Cantalapiedra F, Minguez MT, Valero ML, Sanchez del Pino MM, Munoz-Antoli C, Toledo R, Bernal D.

649 Extracellular vesicles from parasitic helminths contain specific excretory/secretory
650 proteins and are internalized in intestinal host cells. PLoS One. 2012;7:e45974.
651 16. Marcilla A, Martin-Jaular L, Trelis M, de Menezes-Neto A, Osuna A, Bernal
652 D, Fernandez-Becerra C, Almeida IC, Del Portillo HA. Extracellular vesicles in
653 parasitic diseases. J Extracell Vesicles. 2014;3:25040.
654 17. Coakley G, Maizels RM, Buck AH. Exosomes and other extracellular
655 vesicles: the new communicators in parasite infections. Trends Parasitol.
656 2015;31:477-89.
657 18. Chaiyadet S, Sotillo J, Smout M, Cantacessi C, Jones MK, Johnson MS,
658 Turnbull L, Whitchurch CB, Potriquet J, Laohaviroj M, Mulvenna J, Brindley PJ,
659 Bethony JM, Laha T, Sripa B, Loukas A. Carcinogenic liver fluke secretes
660 extracellular vesicles that promote cholangiocytes to adopt a tumorigenic phenotype. J
661 Infect Dis. 2015;212:1636-45.
662 19. Wang L, Li Z, Shen J, Liu Z, Liang J, Wu X, Sun X, Wu Z. Exosome-like
663 vesicles derived by *Schistosoma japonicum* adult worms mediates M1 type immune-
664 activity of macrophage. Parasitol Res. 2015;114:1865-73.
665 20. Buck AH, Coakley G, Simbari F, McSorley HJ, Quintana JF, Le Bihan T,
666 Kumar S, Abreu-Goodger C, Lear M, Harcus Y, Ceroni A, Babayan SA, Blaxter M,
667 Ivens A, Maizels RM. Exosomes secreted by nematode parasites transfer small RNAs
668 to mammalian cells and modulate innate immunity. Nat Commun. 2014;5:5488.
669 21. Sotillo J, Pearson M, Potriquet J, Becker L, Pickering D, Mulvenna J, Loukas
670 A. Extracellular vesicles secreted by *Schistosoma mansoni* contain protein vaccine
671 candidates. Int J Parasitol. 2016;46:1-5.
672 22. Sato T, Stange DE, Ferrante M, Vries RG, Van Es JH, Van den Brink S, Van
673 Houdt WJ, Pronk A, Van Gorp J, Siersema PD, Clevers H. Long-term expansion of

674 epithelial organoids from human colon, adenoma, adenocarcinoma, and Barrett's
675 epithelium. Gastroenterology. 2011;141:1762-72.
676 23. Sotillo J, Sanchez-Flores A, Cantacessi C, Harcus Y, Pickering D, Bouchery
677 T, Camberis M, Tang SC, Giacomin P, Mulvenna J, Mitreva M, Berriman M, LeGros
678 G, Maizels RM, Loukas A. Secreted proteomes of different developmental stages of
679 the gastrointestinal nematode *Nippostrongylus brasiliensis*. Mol Cell Proteomics.
680 2014;13:2736-51.
681 24. Vaudel M, Barsnes H, Berven FS, Sickmann A, Martens L. SearchGUI: An
682 open-source graphical user interface for simultaneous OMSSA and X!Tandem
683 searches. Proteomics. 2011;11:996-9.
684 25. Vaudel M, Burkhart JM, Zahedi RP, Oveland E, Berven FS, Sickmann A,
685 Martens L, Barsnes H. PeptideShaker enables reanalysis of MS-derived proteomics
686 data sets. Nat Biotechnol. 2015;33:22-4.
687 26. Gotz S, Garcia-Gomez JM, Terol J, Williams TD, Nagaraj SH, Nueda MJ,
688 Robles M, Talon M, Dopazo J, Conesa A. High-throughput functional annotation and
689 data mining with the Blast2GO suite. Nucleic Acids Res. 2008;36:3420-35.
690 27. Finn RD, Clements J, Arndt W, Miller BL, Wheeler TJ, Schreiber F, Bateman
691 A, Eddy SR. HMMER web server: 2015 update. Nucleic Acids Res. 2015;43:W30-8.
692 28. Marchler-Bauer A, Lu S, Anderson JB, Chitsaz F, Derbyshire MK, DeWeese-
693 Scott C, Fong JH, Geer LY, Geer RC, Gonzales NR, Gwadz M, Hurwitz DI, Jackson
694 JD, Ke Z, Lanczycki CJ, Lu F, Marchler GH, Mullokandov M, Omelchenko MV,
695 Robertson CL, Song JS, Thanki N, Yamashita RA, Zhang D, Zhang N, Zheng C,
696 Bryant SH. CDD: a Conserved Domain Database for the functional annotation of
697 proteins. Nucleic Acids Res. 2011;39:D225-9.

698 29. Petersen TN, Brunak S, von Heijne G, Nielsen H. SignalP 4.0: discriminating
699 signal peptides from transmembrane regions. Nat Methods. 2011;8:785-6.
700 30. Howe KL, Bolt BJ, Cain S, Chan J, Chen WJ, Davis P, Done J, Down T, Gao
701 S, Grove C, Harris TW, Kishore R, Lee R, Lomax J, Li Y, Muller HM, Nakamura C,
702 Nuin P, Paulini M, Raciti D, Schindelman G, Stanley E, Tuli MA, Van Auken K,
703 Wang D, Wang X, Williams G, Wright A, Yook K, Berriman M, Kersey P, Schedl T,
704 Stein L, Sternberg PW. WormBase 2016: expanding to enable helminth genomic
705 research. Nucleic Acids Res. 2016;44:D774-80.
706 31. Dobin A, Davis CA, Schlesinger F, Drenkow J, Zaleski C, Jha S, Batut P,
707 Chaisson M, Gingeras TR. STAR: ultrafast universal RNA-seq aligner.
708 Bioinformatics. 2013;29:15-21.
709 32. Schmieder R, Lim YW, Edwards R. Identification and removal of ribosomal
710 RNA sequences from metatranscriptomes. Bioinformatics. 2012;28:433-5.
711 33. Altschul SF, Madden TL, Schaffer AA, Zhang J, Zhang Z, Miller W, Lipman
712 DJ. Gapped BLAST and PSI-BLAST: a new generation of protein database search
713 programs. Nucleic Acids Res. 1997;25:3389-402.
714 34. Friedlander MR, Mackowiak SD, Li N, Chen W, Rajewsky N. miRDeep2
715 accurately identifies known and hundreds of novel microRNA genes in seven animal
716 clades. Nucleic Acids Res. 2012;40:37-52.
717 35. Kozomara A, Griffiths-Jones S. miRBase: annotating high confidence
718 microRNAs using deep sequencing data. Nucleic Acids Res. 2014;42:D68-73.
719 36. Enright AJ, John B, Gaul U, Tuschl T, Sander C, Marks DS. MicroRNA
720 targets in Drosophila. Genome Biol. 2003;5:R1.
721 37. Yates A, Akanni W, Amode MR, Barrell D, Billis K, Carvalho-Silva D,
722 Cummins C, Clapham P, Fitzgerald S, Gil L, Giron CG, Gordon L, Hourlier T, Hunt

723 SE, Janacek SH, Johnson N, Juettemann T, Keenan S, Lavidas I, Martin FJ, Maurel T,
724 McLaren W, Murphy DN, Nag R, Nuhn M, Parker A, Patricio M, Pignatelli M, Rahtz
725 M, Riat HS, Sheppard D, Taylor K, Thormann A, Vullo A, Wilder SP, Zadissa A,
726 Birney E, Harrow J, Muffato M, Perry E, Ruffier M, Spudich G, Trevanion SJ,
727 Cunningham F, Aken BL, Zerbino DR, Flicek P. Ensembl 2016. Nucleic Acids Res.
728 2016;44:D710-6.
729 38. Mi H, Huang X, Muruganujan A, Tang H, Mills C, Kang D, Thomas PD.
730 PANTHER version 11: expanded annotation data from Gene Ontology and Reactome
731 pathways, and data analysis tool enhancements. Nucleic Acids Res. 2016.
732 39. Fabregat A, Sidiropoulos K, Garapati P, Gillespie M, Hausmann K, Haw R,
733 Jassal B, Jupe S, Korninger F, McKay S, Matthews L, May B, Milacic M, Rothfels K,
734 Shamovsky V, Webber M, Weiser J, Williams M, Wu G, Stein L, Hermjakob H,
735 D'Eustachio P. The Reactome pathway Knowledgebase. Nucleic Acids Res.
736 2016;44:D481-7.
737 40. Webber J, Clayton A. How pure are your vesicles? J Extracell Vesicles.
738 2013;2.
739 41. WHO. Preventive chemotherapy in human helminthiasis: coordinated use of
740 anthelminthic drugs in control interventions: a manual for health professionals and
741 programme managers. Available:
742 http://whqlibdoc.who.int/publications/2006/9241547103_eng.pdf. 2006.
743 42. Stephenson LS, Holland CV, Cooper ES. The public health significance of
744 *Trichuris trichiura*. Parasitology. 2000;121 Suppl:S73-95.
745 43. WHO. Deworming for health and development. Report of the third global
746 meeting of the partners for parasite control. Geneva: World Health Organization.
747 2005.

748 44. Anonymous. Schistosomiasis and soil-transmitted helminth infections (World
749 Health Assembly Resolution WHA54.19)
750 http://apps.who.int/gb/archive/pdf_files/WHA54/ea54r19.pdf. 2001.
751 45. Williams SE, Brown TI, Roghanian A, Sallenave JM. SLPI and elafin: one
752 glove, many fingers. Clin Sci (Lond). 2006;110:21-35.
753 46. Scott A, Weldon S, Taggart CC. SLPI and elafin: multifunctional
754 antiproteases of the WFDC family. Biochem Soc Trans. 2011;39:1437-40.
755 47. Wilkinson TS, Roghanian A, Simpson AJ, Sallenave JM. WAP domain
756 proteins as modulators of mucosal immunity. Biochem Soc Trans. 2011;39:1409-15.
757 48. Cantacessi C, Campbell BE, Visser A, Geldhof P, Nolan MJ, Nisbet AJ,
758 Matthews JB, Loukas A, Hofmann A, Otranto D, Sternberg PW, Gasser RB. A
759 portrait of the "SCP/TAPS" proteins of eukaryotes-developing a framework for
760 fundamental research and biotechnological outcomes. Biotechnol Adv. 2009;27:376-
761 88.
762 49. Hansen EP, Kringel H, Williams AR, Nejsum P. Secretion of RNA-
763 Containing Extracellular Vesicles by the Porcine Whipworm, *Trichuris suis*. J
764 Parasitol. 2015;101:336-40.
765 50. Liegeois S, Benedetto A, Garnier JM, Schwab Y, Labouesse M. The V0-
766 ATPase mediates apical secretion of exosomes containing Hedgehog-related proteins
767 in *Caenorhabditis elegans*. J Cell Biol. 2006;173:949-61.
768 51. Tritten L, Clarke D, Timmins S, McTier T, Geary TG. *Dirofilaria immitis*
769 exhibits sex- and stage-specific differences in excretory/secretory miRNA and protein
770 profiles. Vet Parasitol. 2016;232:1-7.
771 52. Zamanian M, Fraser LM, Agbedanu PN, Harischandra H, Moorhead AR, Day
772 TA, Bartholomay LC, Kimber MJ. Release of small rna-containing exosome-like

773 vesicles from the human filarial parasite *Brugia malayi*. PLoS Negl Trop Dis.
774 2015;9:e0004069.
775 53. Sato T, Clevers H. Growing self-organizing mini-guts from a single intestinal
776 stem cell: mechanism and applications. Science. 2013;340:1190-4.
777 54. Frising UC, Stange J, Veldhoen m, Intestinal organoids - a powerful model to
778 study interactionsof the epithelial barrier with its environment. In: Hampton-Reeves S
779 editor. 2014; University of Nottingham, UK: Publisher.
780 55. Nozaki K, Mochizuki W, Matsumoto Y, Matsumoto T, Fukuda M, Mizutani
781 T, Watanabe M, Nakamura T. Co-culture with intestinal epithelial organoids allows
782 efficient expansion and motility analysis of intraepithelial lymphocytes. J
783 Gastroenterol. 2016;51:206-13.
784 56. Andreu Z, Yanez-Mo M. Tetraspanins in extracellular vesicle formation and
785 function. Front Immunol. 2014;5:442.
786 57. Cwiklinski K, de la Torre-Escudero E, Trelis M, Bernal D, Dufresne PJ,
787 Brennan GP, O'Neill S, Tort J, Paterson S, Marcilla A, Dalton JP, Robinson MW. The
788 Extracellular Vesicles of the helminth pathogen, *Fasciola hepatica*: biogenesis
789 pathways and cargo molecules involved in parasite pathogenesis. Mol Cell
790 Proteomics. 2015;14:3258-73.
791 58. Tzelos T, Matthews JB, Buck AH, Simbari F, Frew D, Inglis NF, McLean K,
792 Nisbet AJ, Whitelaw CB, Knox DP, McNeilly TN. A preliminary proteomic
793 characterisation of extracellular vesicles released by the ovine parasitic nematode,
794 *Teladorsagia circumcincta*. Vet Parasitol. 2016;221:84-92.
795 59. de la Torre-Escudero E, Bennett AP, Clarke A, Brennan GP, Robinson MW.
796 Extracellular vesicle biogenesis in helminths: more than one route to the surface?
797 Trends Parasitol. 2016;32:921-9.

798 60. Nishikado H, Fujimura T, Taka H, Mineki R, Ogawa H, Okumura K, Takai T.
799 Cysteine protease antigens cleave CD123, the alpha subunit of murine IL-3 receptor,
800 on basophils and suppress IL-3-mediated basophil expansion. Biochem Biophys Res
801 Commun. 2015;460:261-6.
802 61. Drake LJ, Bianco AE, Bundy DA, Ashall F. Characterization of peptidases of
803 adult *Trichuris muris*. Parasitology. 1994;109 (Pt 5):623-30.
804 62. Cantacessi C, Gasser RB. SCP/TAPS proteins in helminths-where to from
805 now? Mol Cell Probes. 2012;26:54-9.
806 63. Wu XJ, Sabat G, Brown JF, Zhang M, Taft A, Peterson N, Harms A, Yoshino
807 TP. Proteomic analysis of *Schistosoma mansoni* proteins released during in vitro
808 miracidium-to-sporocyst transformation. Mol Biochem Parasitol. 2009;164:32-44.
809 64. Chen J, Hu X, He S, Wang L, Hu D, Wang X, Zheng M, Yang Y, Liang C, Xu
810 J, Yu X. Expression and immune response analysis of *Schistosoma japonicum* VAL-
811 1, a homologue of vespid venom allergens. Parasitol Res. 2010;106:1413-8.
812 65. Tribolet L, Cantacessi C, Pickering DA, Navarro S, Doolan DL, Trieu A, Fei
813 H, Chao Y, Hofmann A, Gasser RB, Giacomin PR, Loukas A. Probing of a human
814 proteome microarray with a recombinant pathogen protein reveals a novel mechanism
815 by which hookworms suppress B-cell receptor signaling. J Infect Dis. 2015;211:416-
816 25.
817 66. Moser JM, Freitas T, Arasu P, Gibson G. Gene expression profiles associated
818 with the transition to parasitism in *Ancylostoma caninum* larvae. Mol Biochem
819 Parasitol. 2005;143:39-48.
820 67. Loukas A, Bethony J, Brooker S, Hotez P. Hookworm vaccines: past, present,
821 and future. Lancet Infect Dis. 2006;6:733-41.

822 68. Caradec J, Kharmate G, Hosseini-Beheshti E, Adomat H, Gleave M, Guns E.
823 Reproducibility and efficiency of serum-derived exosome extraction methods. Clin
824 Biochem. 2014;47:1286-92.
825 69. Kesimer M, Scull M, Brighton B, DeMaria G, Burns K, O'Neal W, Pickles RJ,
826 Sheehan JK. Characterization of exosome-like vesicles released from human
827 tracheobronchial ciliated epithelium: a possible role in innate defense. FASEB J.
828 2009;23:1858-68.
829 70. Valadi H, Ekstrom K, Bossios A, Sjostrand M, Lee JJ, Lotvall JO. Exosome-
830 mediated transfer of mRNAs and microRNAs is a novel mechanism of genetic
831 exchange between cells. Nat Cell Biol. 2007;9:654-9.
832 71. Nguyen DG, Booth A, Gould SJ, Hildreth JE. Evidence that HIV budding in
833 primary macrophages occurs through the exosome release pathway. J Biol Chem.
834 2003;278:52347-54. Epub 2003/10/17.
835 72. Fang Y, Wu N, Gan X, Yan W, Morrell JC, Gould SJ. Higher-order
836 oligomerization targets plasma membrane proteins and HIV gag to exosomes. PLoS
837 Biol. 2007;5:e158.
838 73. Krishnamoorthy L, Bess JW, Jr., Preston AB, Nagashima K, Mahal LK. HIV-
839 1 and microvesicles from T cells share a common glycome, arguing for a common
840 origin. Nat Chem Biol. 2009;5:244-50.
841 74. Shen B, Wu N, Yang JM, Gould SJ. Protein targeting to
842 exosomes/microvesicles by plasma membrane anchors. J Biol Chem.
843 2011;286:14383-95.
844 75. Cai J, Han Y, Ren H, Chen C, He D, Zhou L, Eisner GM, Asico LD, Jose PA,
845 Zeng C. Extracellular vesicle-mediated transfer of donor genomic DNA to recipient

846 cells is a novel mechanism for genetic influence between cells. J Mol Cell Biol.
847 2013;5:227-38.
848 76. Daugaard I, Hansen TB. Biogenesis and Function of Ago-Associated RNAs.
849 Trends Genet. 2017.
850 77. McSorley HJ, Loukas A. The immunology of human hookworm infections.
851 Parasite Immunol. 2010;32:549-59.
852
853 **Figure legends**
854 **Figure 1. Bioinformatic analyses of the proteins secreted by *Trichuris muris***. (A)
855 Bar graph showing the most abundant protein families after a Pfam analysis on the
856 excretory/secretory proteins derived from *T. muris*. (B) Bar graph showing the most
857 abundantly represented gene ontology molecular function terms in excretory/secretory
858 proteins derived from *T. muris*.
859
860 **Figure 2. Tunable resistive pulse sensing analysis of the extracellular vesicles**
861 **(EVs) secreted by *Trichuris muris*.** (A) The size and number of the EVs secreted by
862 *T. muris* after purification using an Optiprep® gradient was analysed using a qNano
863 system (iZon). (B) Logarithmic plot highlighting the smaller numbers of vesicles in
864 fractions 7-10. Only fractions 4-10 contained enough vesicles for the analyses.
865
866 **Figure 3. *Trichuris muris* extracellular vesicles (EVs) are internalized by murine**
867 **colonic organoids.** (A) Representative fluorescence images of PKH-26-labelled EVs
868 (red) internalized by organoids after 3 hours at 37°C and 4°C (metabolically inactive
869 cells). Hoechst dye (blue) was used to label cell nuclei. † indicates the lumen of the
870 organoids, which corresponds to the murine gut lumen, separated by the dotted line

from the epithelial cell layer. White bar corresponds to 20 μm. (B) Magnification of the framed area in A. White bar corresponds to 10 μm. (C) Percentage of the corrected total fluorescence (CTF) adjusted by background fluorescence and the surveyed area of PKH26-stained EVs in total epithelial cells (donut-shaped selection) or in the lumen incubated under different conditions in 10 different organoids from 2 technical replicates (5 each). *** indicates highly significant results ($p<0.001$). Error bars indicate 95% confidence intervals.

Figure 4. Gene ontology analysis of proteins from the extracellular vesicles (EVs) secreted by *Trichuris muris*. (A) Bar graph showing the most abundantly represented gene ontology biological process terms in proteins present in the EVs secreted by *T. muris*. (B) Bar graph showing the most abundantly represented gene ontology molecular function terms in proteins present in the EVs secreted by *T. muris.*

Figure 5. Analysis of the 475 full-length mRNAs detected in *Trichuris muris* extracellular vesicles. (A) Bar graph showing the most represented protein families (Pfam) from the translated mRNAs. (B) Molecular functions and (C) biological functions of proteins encoded by each of the 475 transcripts assigned to gene ontology functional annotation.

Figure 6. Prediction of *T. muris* extracellular vesicle (EV) miRNA target interactions to murine host genes. Functional map of *T. muris* EV miRNAs and their target murine host genes. (A) Individual targeted host genes are categorized by PantherDB signaling pathway analysis (heat map corresponds to individual targeted genes in the murine host). Bottom axis shows the 56 identified miRNAs in *T. muris*

EVs and their abundances (average mean read counts from two biological replicates), termed according to their closest homologues (*de novo* transcripts were designated as tmu.miR.ev#). Total number of targeted genes identified by PantherDB categories classified as (B) 'immune system related', (C) 'receptor regulation', and (D) 'transcription regulation'.

Supplementary Figure 1. Prediction of *T. muris* extracellular vesicle (EV) miRNA target interactions to murine host genes. Functional map of *T. muris* EV miRNAs and their target murine host genes categorized by PantherDB signalling, metabolic, disease, and other pathways. Heat map corresponds to individual targeted genes in the murine host.

Supplementary Table 1. Detailed analysis of the proteins secreted by *Trichuris muris*. Proteins were annotated using Blast2GO [26], and the description blast e-values, gene ontology (GO) terms and enzyme codes are shown. Information about the number of unique peptides, peptide-spectrum matches (PSM), spectrum counting and coverage is also provided for each protein and batch analysed.

Supplementary Table 2. Signal peptide analysis of the proteins secreted by *Trichuris muris*. An analysis to check for the presence of a signal peptide in each of the proteins secreted by *T. muris* was performed using SignalP [29].

Supplementary Table 3. Proteomic analysis of extracellular vesicles (EVs) secreted by *Trichuris muris*. Details of the identification of the proteins present in the EVs secreted by *T. muris* using X!Tandem, Tide, MS-GF + and OMSSA. All

proteins are shown, including contaminants, and independently of the number of unique peptides identified.

Supplementary Table 4. Curated proteomic analysis of extracellular vesicles (EVs) secreted by *Trichuris muris*. Proteins are sorted by theoretical abundance (spectrum counting). Only proteins from *T. muris* or *Mus musculus* are shown.

Supplementary Table 5. Data on 475 detected mRNA transcripts from *T. muris* extracellular vesicles. RNA-seq data was aligned to the *T. muris* reference genome models [30] and the E-value of the alignment, the fragments per kilobase of exon model per million mapped reads (FPKM) normalized by the length of the gene and the relative coverage of the alignment are provided.

Supplementary Table 6. Data description on predicted *T. muris* miRNA-host target interactions. Table showing the 56 miRNAs identified in the *T. muris* extracellular vesicles and their 2,043 3'UTR predicted binding sites in the mouse genome.

938 **Table 1. Features of the different fractions isolated after Optiprep fractionation**
939 **of extracellular vesicles from *Trichuris muris*.** Despite protein being detected in all
940 fractions, only vesicles from fractions 4-10 could be quantified. The purity of the
941 different fractions was calculated according to [40].
942

Optiprep fraction	Density (g/mL)	Protein quantification (µg/ml)	Particle concentration (particles/mL)	Purity of vesicles particles/µg	Particle size nm
S1	1.04	104.69	-	-	-
S2	1.05	290.10	-	-	-
S3	1.05	435.58	-	-	-
S4	1.06	477.86	2.96E+08	6.19E+05	93±41.5
S5	1.07	474.19	7.47E+10	1.58E+08	72±11.7
S6	1.07	310.61	1.34E+12	4.31E+09	72±23.8
S7	1.08	202.99	8.21E+10	4.04E+08	90±25.5
S8	1.10	160.76	1.31E+10	8.15E+07	152±75.3
S9	1.12	190.46	1.31E+10	6.88E+07	183±68.2
S10	1.15	436.86	1.71E+09	3.91E+06	165±54.9
S11	1.21	232.77	-	-	-
S12	1.27	83.35	-	-	-

943

A

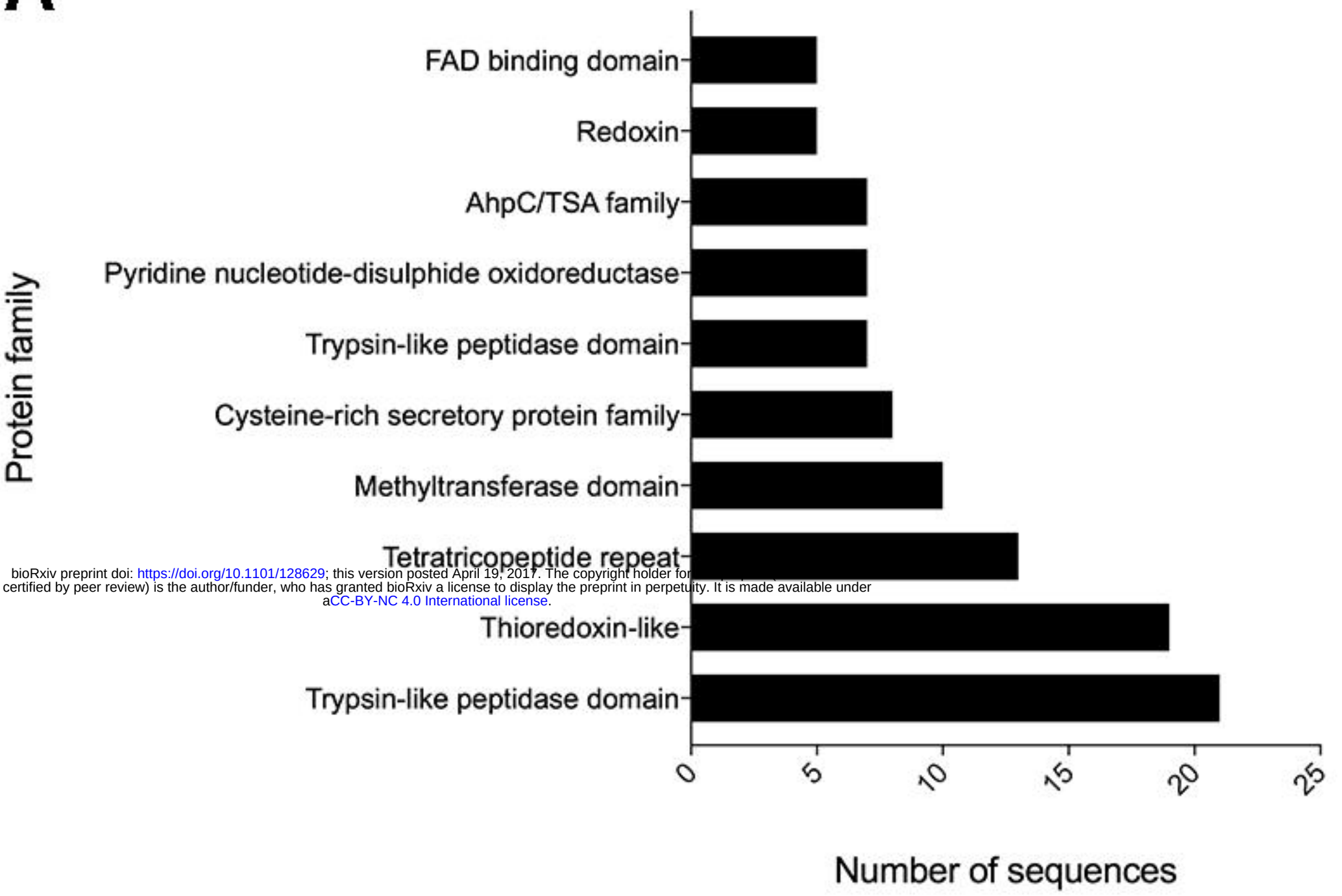

B

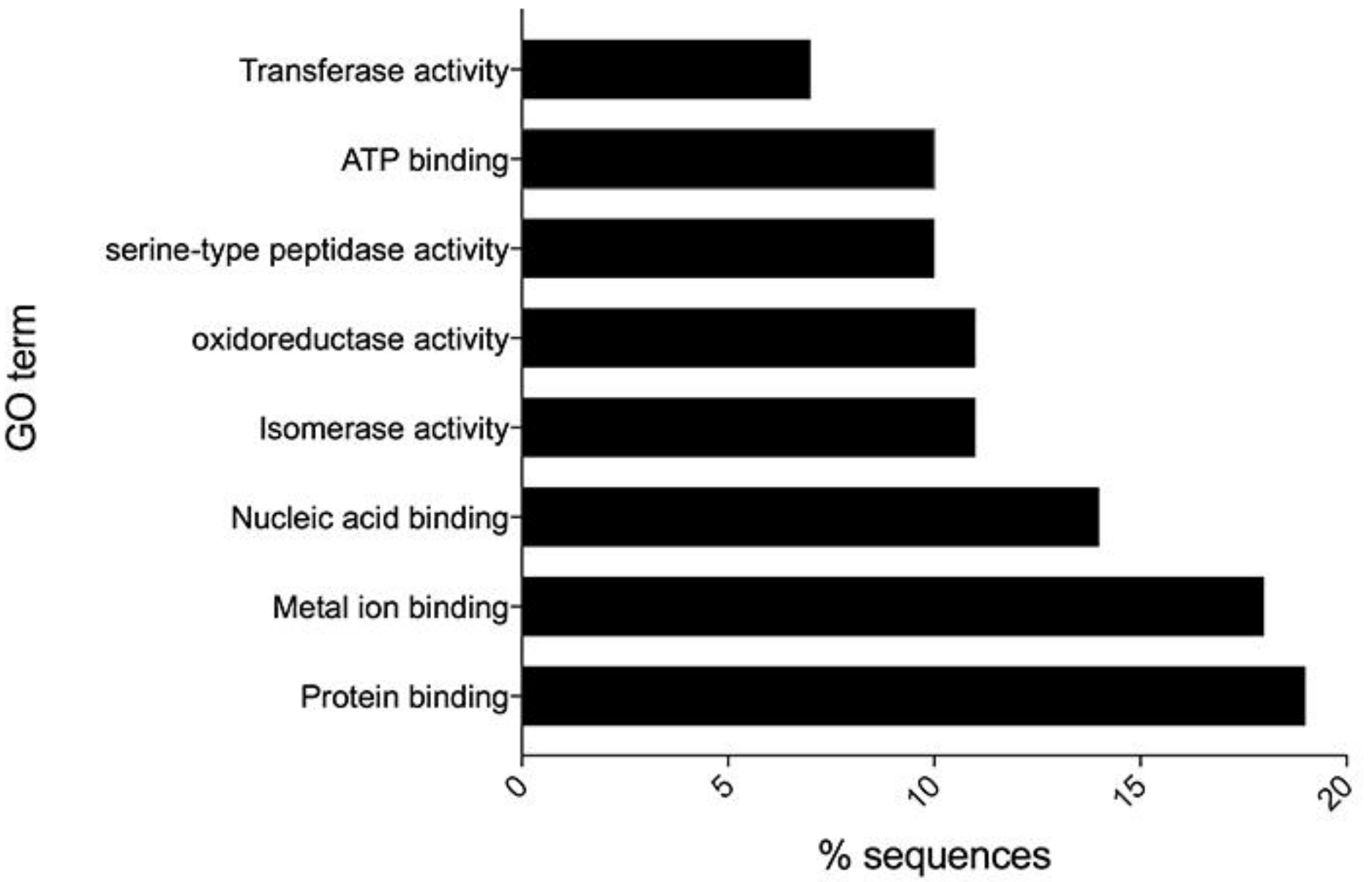

A

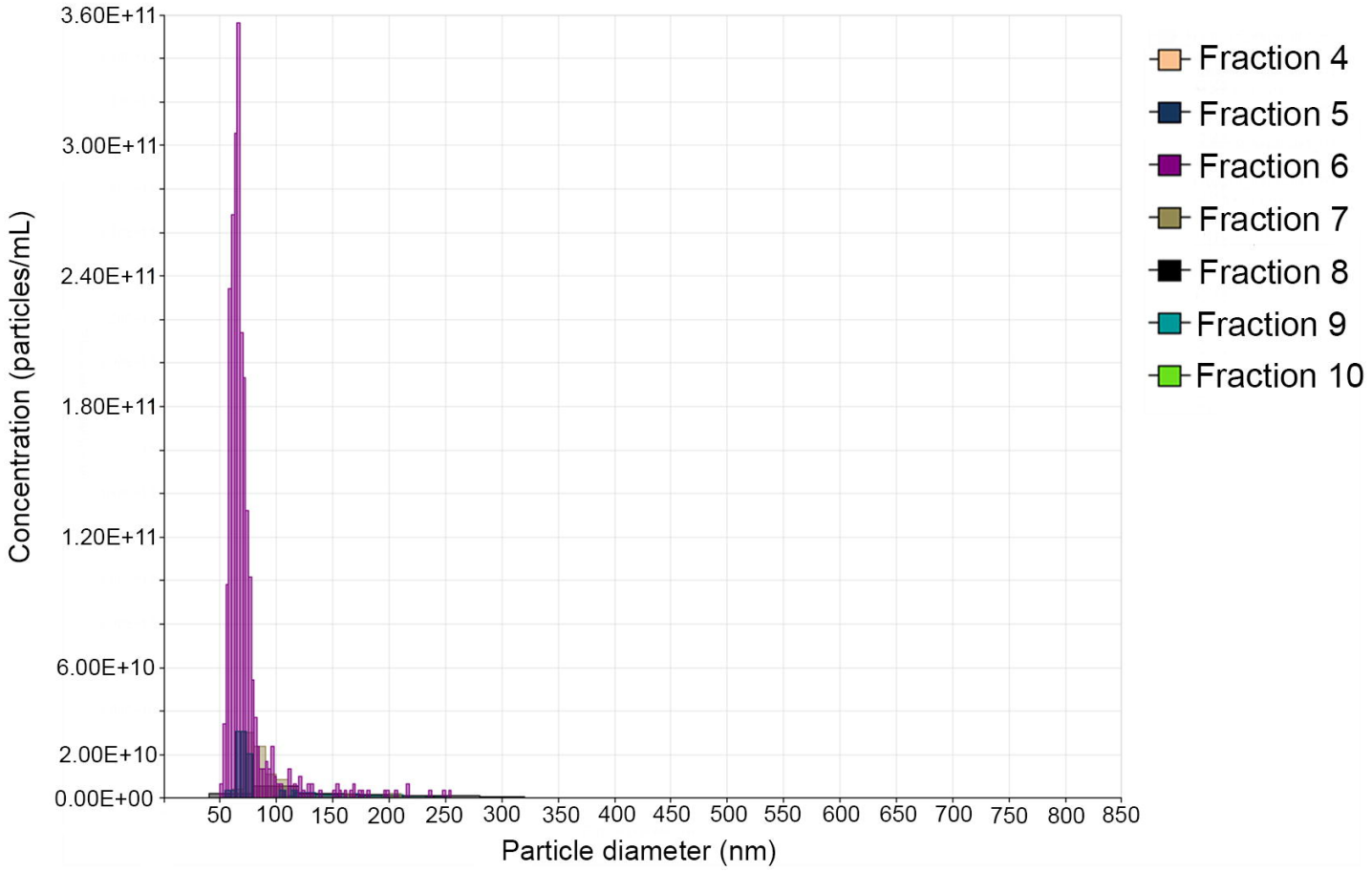
3.60E+11
3.00E+11
2.40E+11
1.80E+11
1.20E+11
6.00E+10
2.00E+10
0.00E+00
Concentration (particles/mL)
50 100 150 200 250 300 350 400 450 500 550 600 650 700 750 800 850
Particle diameter (nm)
Fraction 4
Fraction 5
Fraction 6
Fraction 7
Fraction 8
Fraction 9
Fraction 10

B

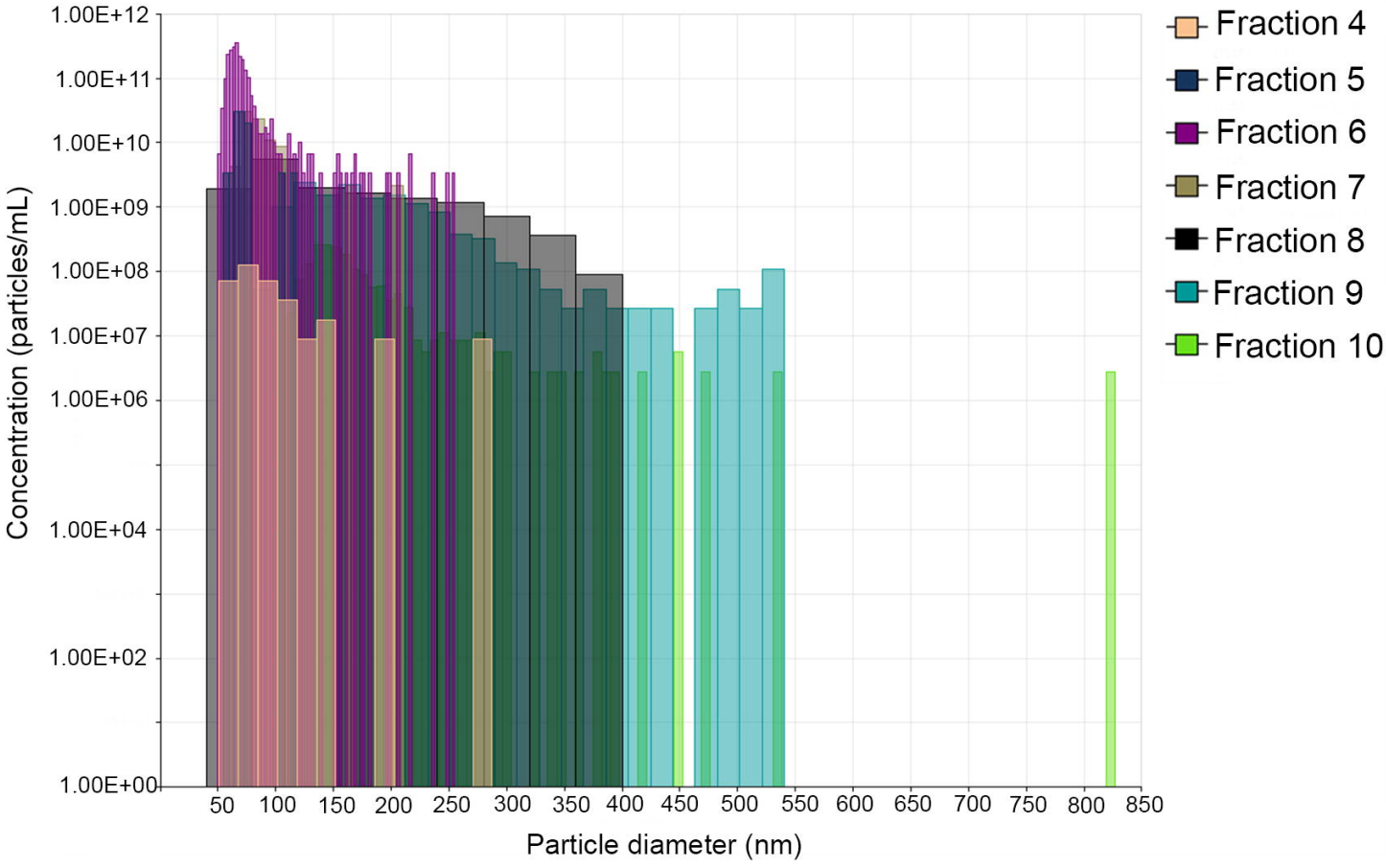
1.00E+12
1.00E+11
1.00E+10
1.00E+09
1.00E+08
1.00E+07
1.00E+06
1.00E+04
1.00E+02
1.00E+00
Concentration (particles/mL)
50 100 150 200 250 300 350 400 450 500 550 600 650 700 750 800 850
Particle diameter (nm)
Fraction 4
Fraction 5
Fraction 6
Fraction 7
Fraction 8
Fraction 9
Fraction 10

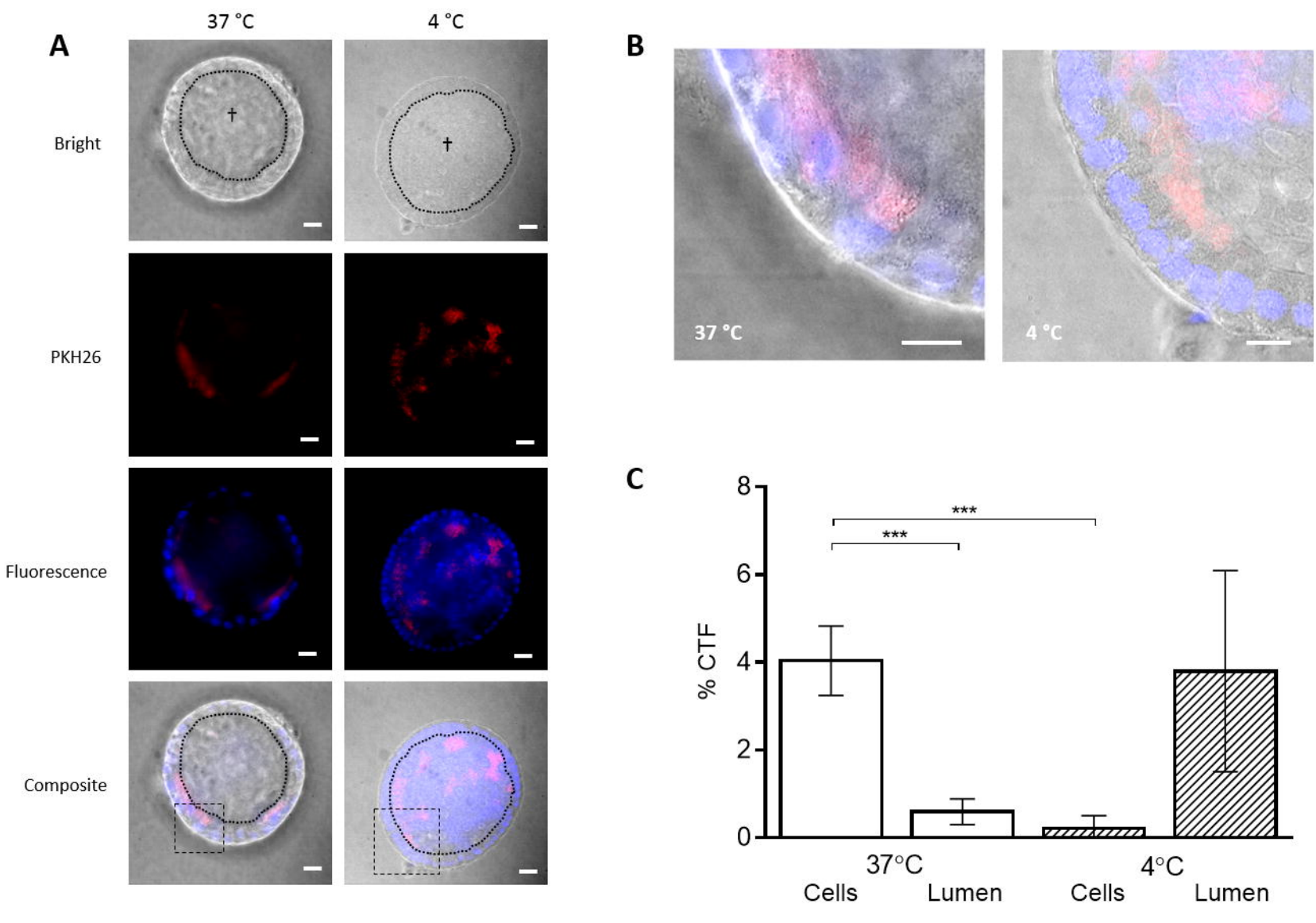
A
37 °C
4 °C
Bright
PKH26
Fluorescence
Composite
B
37 °C
4 °C
C
% CTF
8
6
4
2
0
***
***
37°C
4°C
Cells
Lumen
Cells
Lumen

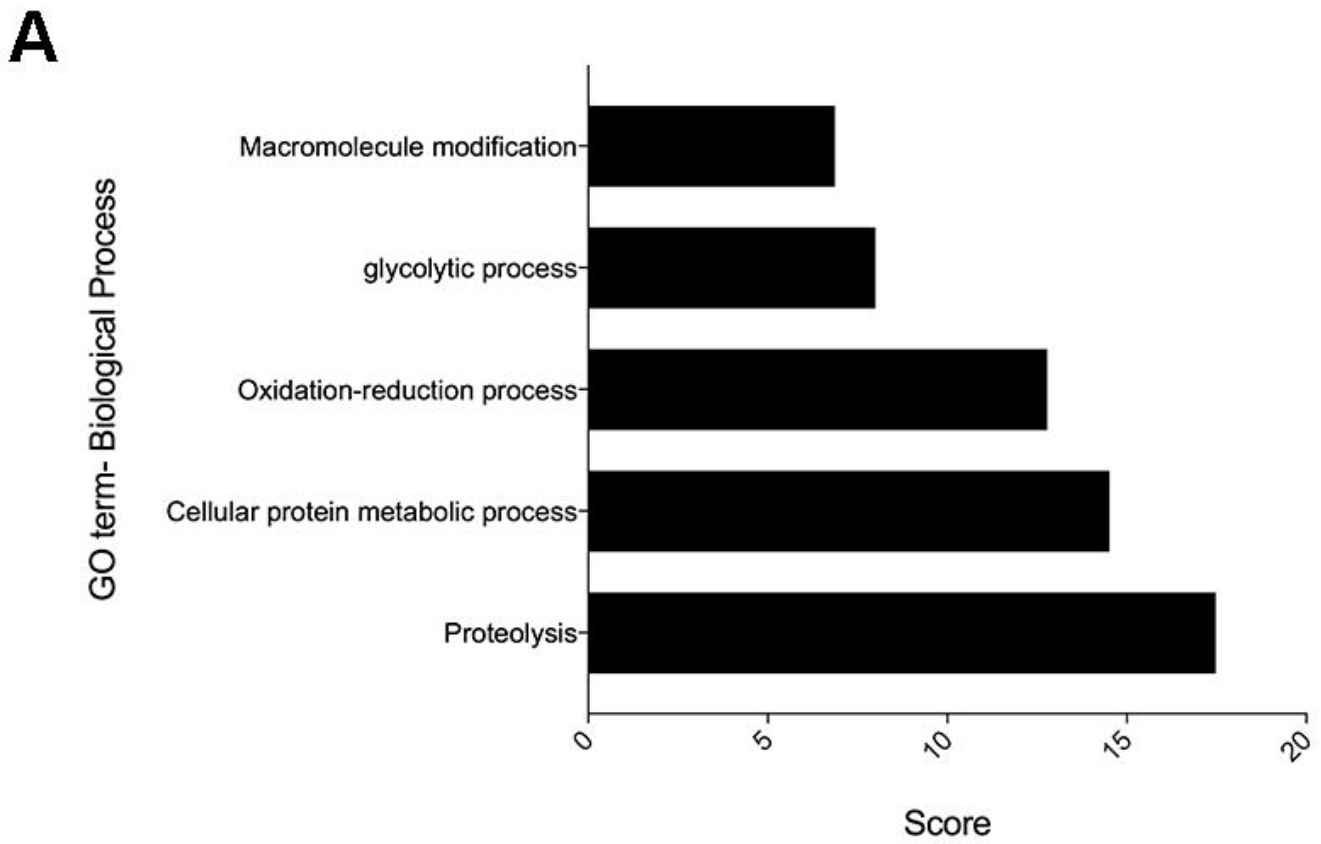
A
GO term- Biological Process
Macromolecule modification
glycolytic process
Oxidation-reduction process
Cellular protein metabolic process
Proteolysis
0
5
10
15
20
Score

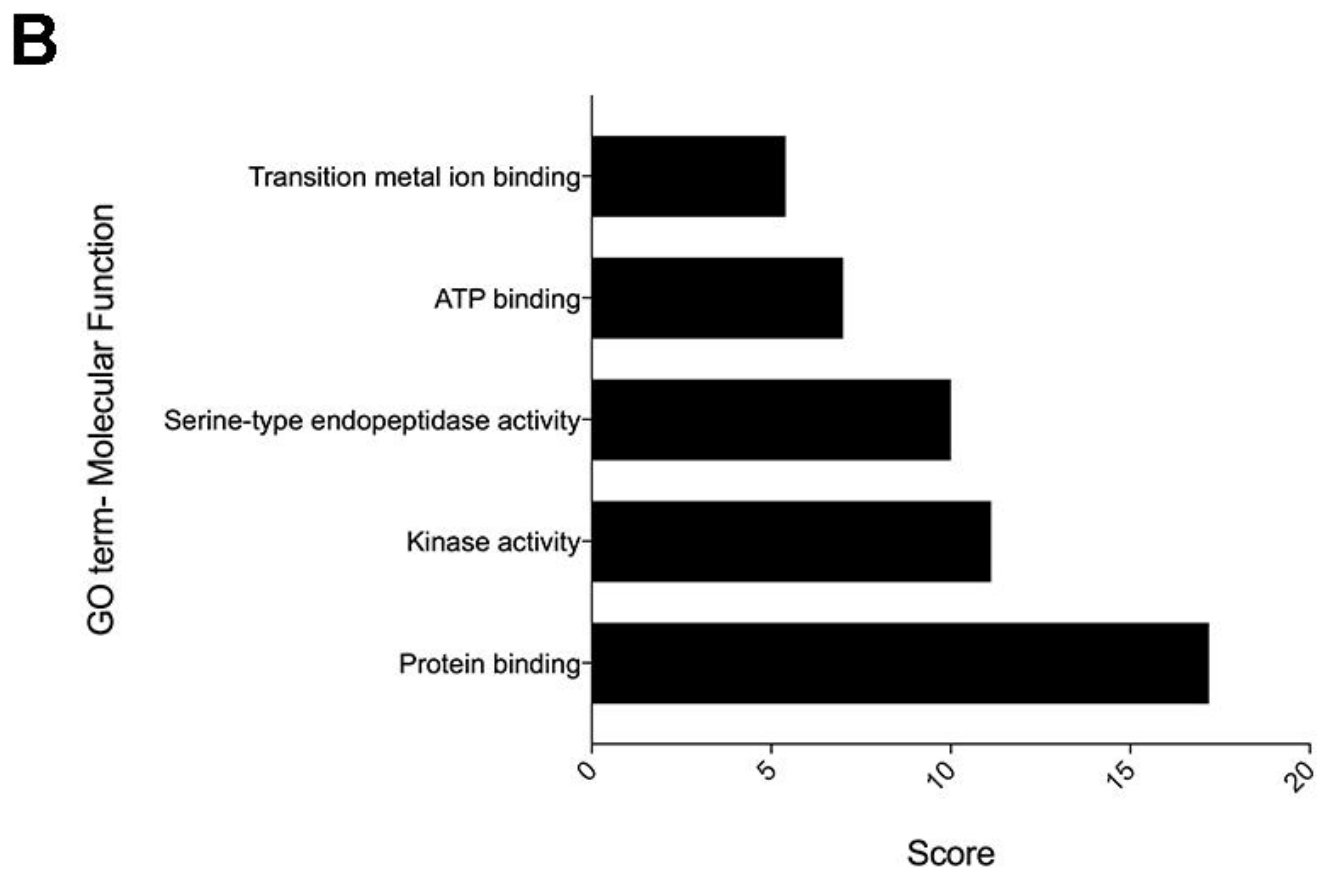
B
GO term- Molecular Function
Transition metal ion binding
ATP binding
Serine-type endopeptidase activity
Kinase activity
Protein binding
0
5
10
15
20
Score

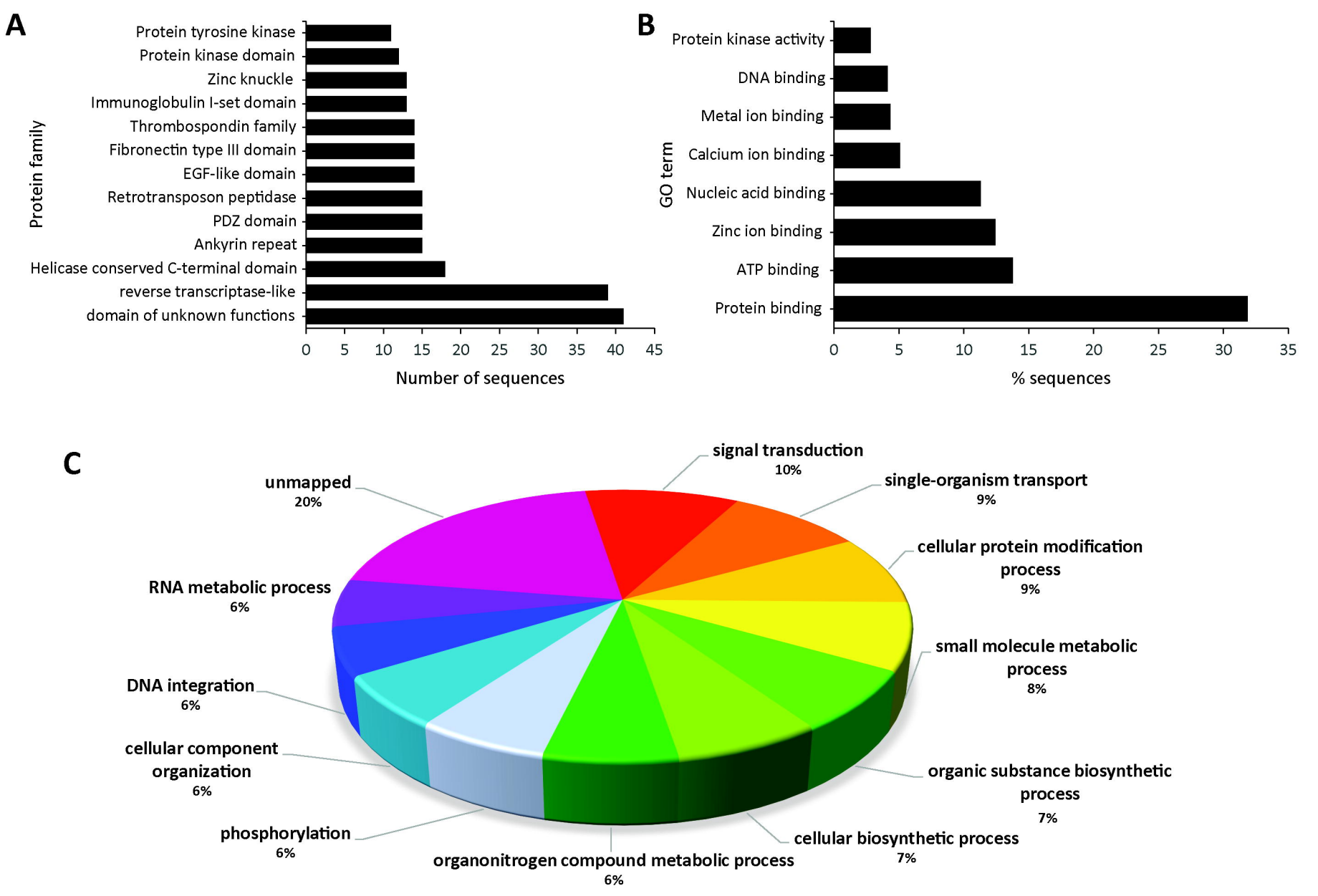
A
Protein tyrosine kinase
Protein kinase domain
Zinc knuckle
Immunoglobulin I-set domain
Thrombospondin family
Fibronectin type III domain
EGF-like domain
Retrotransposon peptidase
PDZ domain
Ankyrin repeat
Helicase conserved C-terminal domain
reverse transcriptase-like
domain of unknown functions
Protein family
0 5 10 15 20 25 30 35 40 45
Number of sequences
B
Protein kinase activity
DNA binding
Metal ion binding
Calcium ion binding
Nucleic acid binding
Zinc ion binding
ATP binding
Protein binding
GO term
0 5 10 15 20 25 30 35
% sequences
C
signal transduction 10%
single-organism transport 9%
cellular protein modification process 9%
small molecule metabolic process 8%
organic substance biosynthetic process 7%
cellular biosynthetic process 7%
organonitrogen compound metabolic process 6%
phosphorylation 6%
cellular component organization 6%
DNA integration 6%
RNA metabolic process 6%
unmapped 20%

A

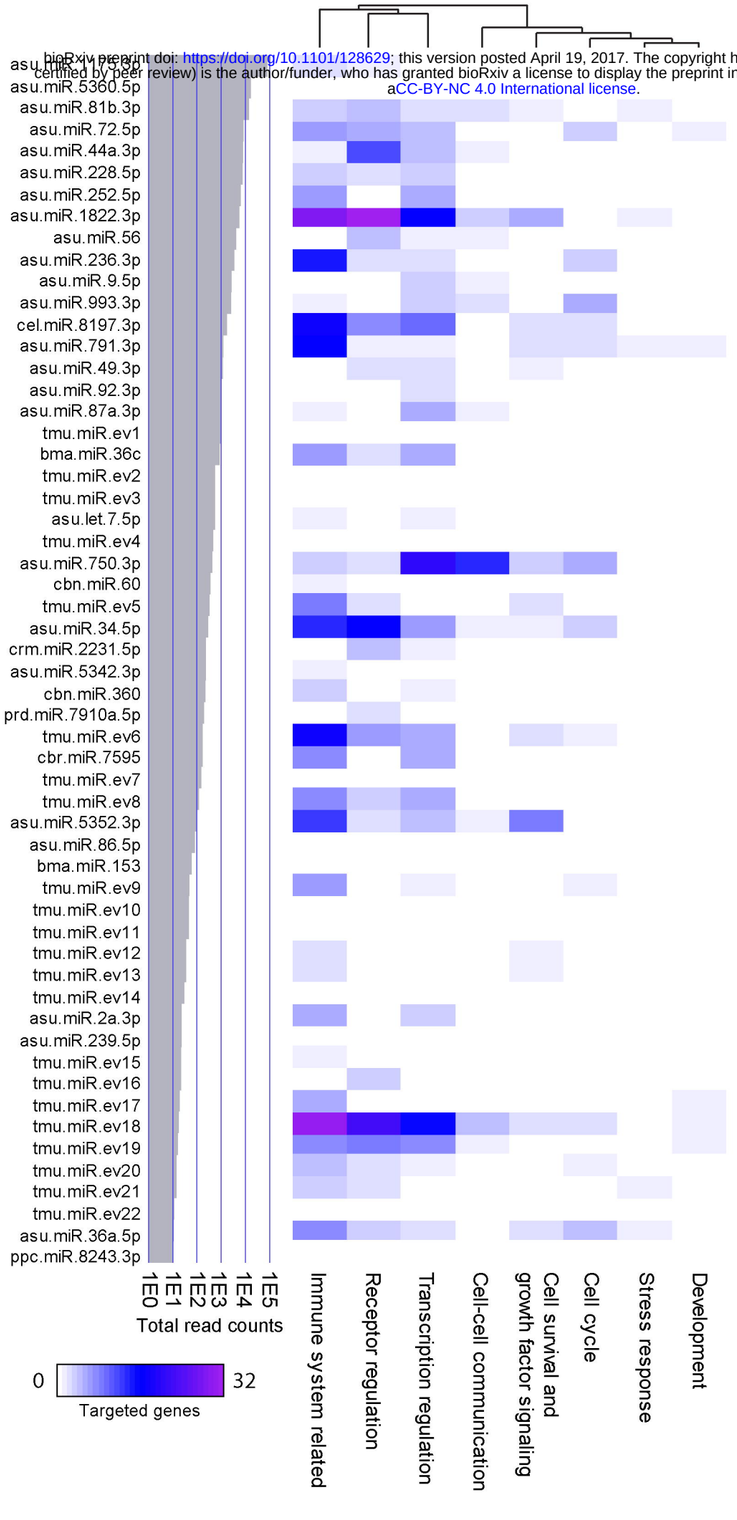

B

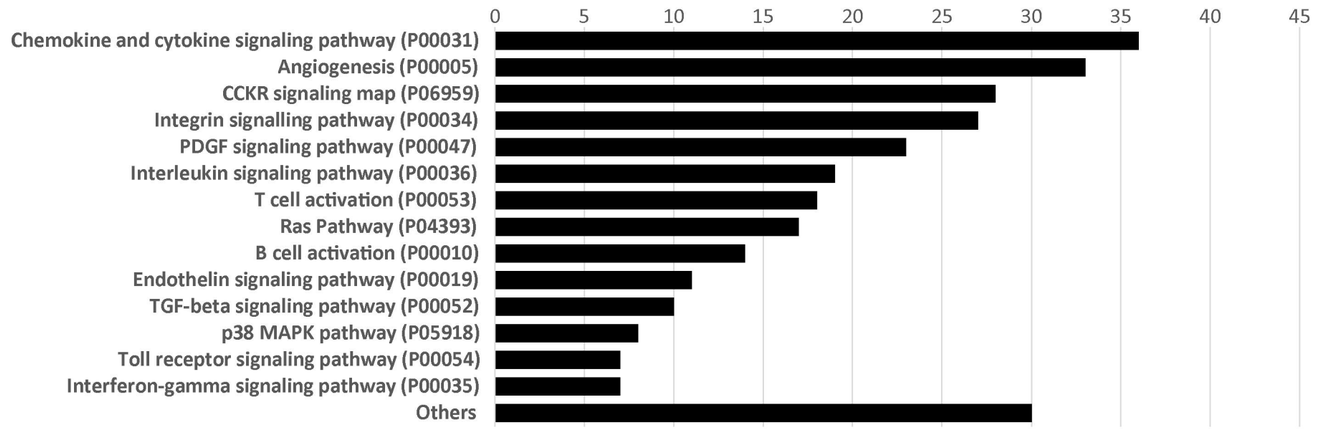

C

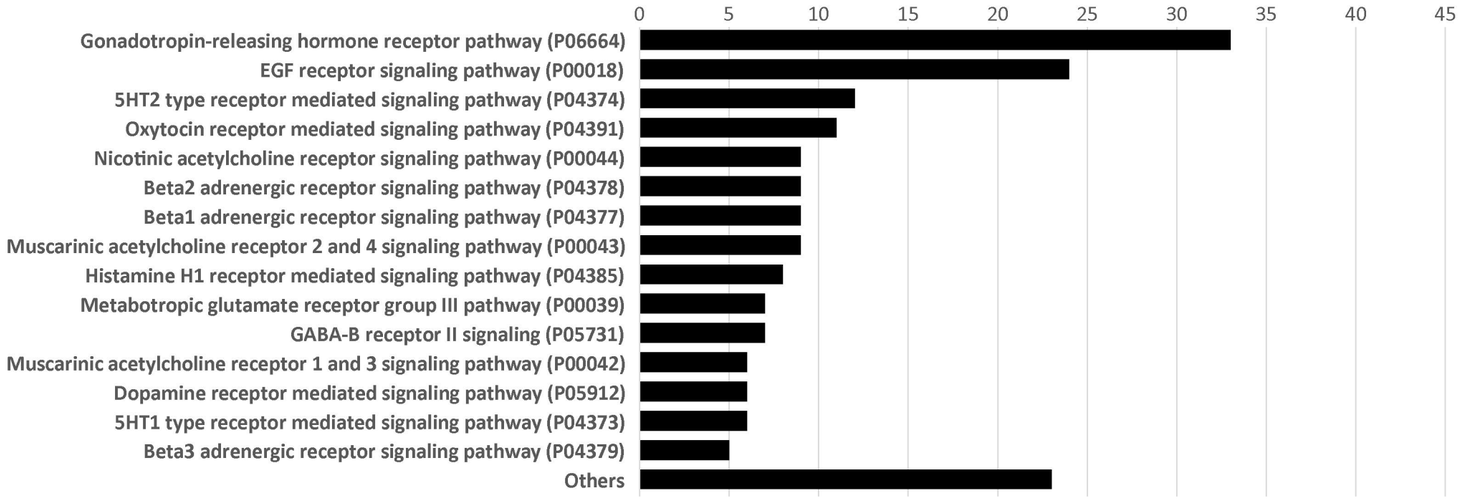

D